Dynamic traffic assignment in degradable networks: Paradoxes and formulations with stochastic link transmission model

Jiancheng Long
Professor
School of Automotive and Transportation Engineering
Hefei University of Technology
Hefei 230009, China
Tel: +86-551-63831101
E-mail: jianchenglong@hfut.edu.cn

W.Y. Szeto
Associate Professor
Department of Civil Engineering
The University of Hong Kong
Pokfulam Road, Hong Kong
Tel: +852-28578552
Email: ceszeto@hku.hk

Jianxun Ding
Associate Professor
School of Automotive and Transportation Engineering
Hefei University of Technology
Hefei 230009, China
E-mail: dingjianxun@hfut.edu.cn

September 1, 2017
Paper revised and resubmitted to Transportmetrica B

Abstract:

This paper proposes a simultaneous route and departure time choice (SRDTC) problem with fixed demand in a degradable transport network. In this network, travelers face with stochastic travel times. Their selection of routes and departure times follows the UE principle in terms of the mean generalized route cost, which is defined as the probabilistic dynamic user optimal (PDUO) principle. The proposed PDUO-SRDTC problem is formulated as a variational inequality (VI) problem. As a special case of PDUO-SRDTC problem, the PDUO route choice (PDUO-RC) problem is also proposed and formulated as a VI problem. Network degradation is defined on the degradation of the outflow capacity of each link. A Monte–Carlo-based stochastic link transmission model (MC-SLTM) is developed to capture the effect of physical queues and the random evolution of traffic states during flow propagation to estimate mean generalized route costs. Both the extragradient algorithm and the route-swapping method with a variable sample size scheme are developed to solve the proposed VI problems. Numerical examples are developed to illustrate the paradoxical phenomena of the problems and the effectiveness of the solution methods. Numerical results show that constructing a new road, enhancing link outflow capacity, or reducing outflow capacity degradation can lead to poor network performance and it is important to consider both network degradation and queue spillback when making transportation policies aimed at improving network performance. The results also demonstrate that the variable sample size scheme can give a quicker and better solution than the traditional fixed sample size scheme.

Keywords: Dynamic traffic assignment; degradable network; probabilistic dynamic user optimal; stochastic link transmission model; paradoxes.

1. Introduction

Dynamic traffic assignment (DTA) models are widely used tools for off-line network planning and policy evaluations as well as online traffic operation and management. They consist of two main components: travel choice principle and traffic flow component (Szeto and Lo, 2006).

The travel choice principle depicts travelers' propensity to travel, e.g., how they select their routes, departure times, modes, or destinations. The most commonly used travel choice principles in the DTA literature mainly include the dynamic user optimal (DUO) principle (e.g., Ran and Boyce, 1996; Lo and Szeto, 2002; Huang and Lam, 2002; Nie and Zhang, 2010; Long et al., 2013b, 2016b; Ge et al., 2015a), the stochastic DUO (SDUO) principle, (e.g., Lim and Heydecker, 2005; Szeto et al., 2011; Meng and Khoo, 2012; Long et al., 2015a), and the dynamic system optimal principle (e.g., Merchant and Nemhauser, 1978a,b; Ziliaskopoulos, 2000; Nie, 2011; Han et al., 2013b; Zhu and Ukkusuri, 2013; Long et al., 2016b). The DUO/SDUO/dynamic system optimal principle assumes that travelers select their routes and/or departure times to minimize their actual/perceived/marginal travel costs. All above three principles assume that once all travelers have made travel choice decision(s), i.e., once the route flow of the network is determined, their travel times/costs are deterministic. However, in fact, travelers' travel times are usually uncertain due to the effects of random events, such as traffic incidents and traffic signal failures. To capture more realistic travel behavior, the extended travel choice principles are proposed in the literature, e.g., reliability-based DUO (Li et al., 2015), reliability-based SDUO (Szeto et al., 2011), and probabilistic dynamic user optimal (PDUO) (Fosgerau, 2010; Xiao et al., 2015). Each principle has different behavioral assumptions that need to be verified for the dataset used (Szeto and Wong, 2012).

According to the travel choice dimension considered in the travel choice principle, DTA problems can be broadly classified into three categories (Szeto and Wong, 2012): (1) the pure departure time choice problems (e.g., Vickrey, 1969; Arnott et al., 1990; Lindsey, 2004; Siu and Lo, 2013; Xiao et al., 2015), (2) the pure route choice problems (e.g., Lo and Szeto, 2002; Mounce and Carey, 2011; Zheng and Chang, 2011; Carey and Ge, 2012; Han et al., 2013a; Long et al., 2013b, 2015a, 2016a; Ge et al., 2015a; Jiang et al., 2016), and (3) the simultaneous route and departure time choice (SRDTC) problems (e.g., Friesz et al., 1993; Ran and Boyce, 1996; Huang and Lam, 2002; Szeto and Lo, 2004; Lim and Heydecker, 2005; Zhang et al., 2008; Han et al., 2013b; Han et al., 2015, 2016; Long et al., 2015b, 2016b). The first two categories of DTA problems are special cases of the last category of problems.

The traffic flow component of DTA models depicts how traffic propagates inside a traffic network and hence governs the network performance in terms of travel time (Szeto and Wong, 2012). The procedure in implementation is often referred to as dynamic network loading (DNL). The traffic flow component in DTA models can be distinguished by four main existing approaches: exit functions (e.g., Merchant and Nemhauser,

1978a,b; Carey and Srinivasan, 1993; Huang and Lam, 2002), link performance functions (e.g., Ran and Boyce, 1996; Nie and Zhang, 2005), the point queue (bottleneck) model (e.g., Kuwahara, 1990; Kuwahara and Akamatsu, 1997); and the Lighthill and Whitham (1955) and Richards (1956) (LWR) hydrodynamic model (e.g., Ziliaskopoulos, 2000; Lo and Szeto, 2002; Szeto and Lo, 2004; Zhu and Ukkusuri, 2013; Chow et al., 2015; Ge et al., 2015b, Han et al., 2016). The first three approaches have a simpler calculation but fail to capture some fundamental traffic dynamics such as queue spillback. The last approach can describe dynamic traffic conditions on a road network, including shock waves and the propagation of queues over links. This approach often relies on either Daganzo's (1995) solution scheme (i.e., the cell transmission model (CTM)) or Newell's (1993) solution scheme (see Kuwahara and Akamatsu, 2001; Lo and Szeto, 2002; Yperman, 2007; Long et al., 2015a, 2016a for example) to perform DNL.

In the literature, the traffic flow models in DTA models are mainly developed for deterministic road networks (see Mun, 2007 for a comprehensive review). Only a few existing DNL models are developed for stochastic road networks. For example, the stochastic CTM (SCTM) proposed by Sumalee et al. (2011) to model traffic density on freeway segments with stochastic demand and supply. Szeto et al. (2011) proposed a Monte-Carlo-based SCTM to capture the effect of physical queues and the random evolution of traffic states during flow propagation. The link transmission model (LTM), which is developed mainly based on Newell's solution scheme, has not been extended for stochastic road networks although it is more computationally efficient than the CTM.

There are three categories of methods to obtain travel times in stochastic road networks: (1) exact methods (e.g., Fosgerau, 2010; Xiao et al., 2015), (2) analytical approximation methods (e.g., Lo and Tung, 2003; Lo et al., 2006; Sumalee et al. 2011; Li et al., 2015), and (3) Monte Carlo Simulation (MCS) methods (e.g., Szeto et al., 2011; Meng and Liu, 2012; Liu and Meng, 2013). The first category can obtain the exact mean and standard deviation of travel times/costs but is only available for some simple networks. The second category adopts approximate schemes to estimate the mean and standard deviation of travel times/costs. Computational efficiency is the major merit of this category of methods. However, their applications are usually limited to some specified distributions for the stochastic variables and the accuracy of the estimated travel times/costs cannot be ensured. The accuracy of the third category, i.e., MCS methods, is determined by the sample size. The larger the sample size is adopted, the higher accuracy the MCS methods can guarantee. Theoretically, an MCS method is exact if the sample size is infinite. Therefore, if the sample size is large enough, MCS methods can be more accurate than analytical approximation methods. Another merit of the MCS methods is that the stochastic variables can be defined by any distributions.

In this paper, we propose a PDUO-SRDTC problem with fixed demand in a transport network with road outflow capacity degeneration, which adds variability to travelers' travel times. We assume that travelers are aware of the road outflow capacity degeneration probability and their route and departure time choice follows

the UE principle in terms of the mean generalized route travel cost (Fosgerau, 2010; Xiao et al., 2015), i.e., the PDUO principle. As a special case of the PDUO-SRDTC problem, the PDUO route choice (PDUO-RC) problem is also proposed. Both the PDUO-SRDTC and PDUO-RC problems are formulated as variational inequality (VI) problems. Because of the computational efficiency of the LTM and its ability to capture queue spillback and shockwave phenomena, we propose a Monte–Carlo-based stochastic LTM (MC-SLTM) to depict the traffic flow propagation in degradable transport networks. The MC-SLTM relies on an MCS to generate traffic states for DNL and collect travel time/cost statistics from each DNL. In the MC-SLTM, link outflow capacities are modeled as random variables, which can be defined by any distributions.

The proposed DTA problems are formulated as VI problems, which can be solved by any general computational technique developed for VI problems, provided that the convergent requirements are satisfied. In this paper, both the extragradient method (Long et al., 2013b, 2016b; Jiang et al., 2016) and the route swapping method (Huang and Lam, 2002; Szeto and Lo, 2006; Tian et al., 2012; Long et al., 2016b) are modified to solve the proposed DTA models. To speed up the computation, the sample size of the MC-SLTM incorporated into the two solution methods can vary from iteration to iteration. To our best knowledge, both the route-swapping method and the extragradient method have not been used to solve stochastic network assignment problems including ours, and hence the performance of the two revised methods for solving these problems has not been known yet. Therefore, numerical examples are set up to illustrate the performance of the solution methods.

The proposed models can also be used to evaluate the performance of a network design. In fact, one important application of any DTA model is to evaluate network design strategies, such as proposals to improve the system performance through new links or improving the outflow capacity of an existing link. To the best of our knowledge, little effort (Zhang et al., 2008) has been spent on investigating whether a Braess-like paradox actually exists in DTA with physical queues and no studies are on examining whether a Braess-like paradox actually exists in DTA in a degradable network. Therefore, in this paper, examples are set up to illustrate the paradoxical phenomena of the proposed DTA problems not discussed in the literature, with the emphasis on network degradation and queue spillback.

The main contributions of our research are as follows.

First, we propose a PDUO-SRDTC problem and its special case, i.e., a PDUO-RC problem, in a degradable road network, and provide VI formulations for the proposed DTA problems.

Second, we develop an MC-SLTM to capture both the effect of physical queues and the random evolution of traffic states during flow propagation and to estimate the mean generalized route travel costs.

Third, we introduce the concept of variable sample size in an MCS and based upon this concept, we propose revised solution methods to solve PDUO-SRDTC and PDUO-RC problems to obtain more accurate solutions quicker.

Fourth, we give novel insights into the paradoxical phenomena associated with (dynamic) traffic assignment in degradable networks. In particular, we illustrate that constructing a new road, enhancing link outflow capacity, or reducing outflow capacity degradation can lead to poor network performance.

Fifth, we present a new implication to make transportation policies—physical queue and network degradation must be taken into consideration in any policies aimed towards the reduction in total system travel cost (TSTC).

The remainder of this paper is organized as follows. In the next section, both the PDUO-SRDTC and PDUO-RC problems are formulated as VI problems. Section 3 describes the MC-SLTM. In Section 4, the route swapping method and the extragradient method are extended to solve the proposed DTA models. Numerical examples are given in Section 5, and finally, a conclusion is provided in Section 6.

2. Model formulation

2.1. Notations

We consider a network $G(N, A)$ with multiple origins and destinations, where N and A are defined as the set of nodes and the set of arcs (links), respectively. Link $a = (l_a, h_a)$ is the link with the tail node l_a and the head node h_a. $\Gamma(i)$ denotes the set of links whose tail node is i, and $\Gamma^{-1}(i)$ denotes the set of links whose head node is i. R and S denote the set of origin nodes and the set of destination nodes, respectively. We discretize the time period T of interest and the demand period T_d into finite sets of time intervals $K = \{k = 1, 2, \cdots, \underline{K}\}$ and $K_d = \{k = 1, 2, \cdots, \underline{K}_d\}$, respectively. Let δ be the interval length such that $\delta \underline{K} = T$ and $\delta \underline{K}_d = T_d$. Without loss of generality, we let δ = 1. The following notations are adopted throughout this paper:

P^{rs}	set of routes connecting origin-destination (OD) pair (r, s)
$f_p^{rs}(k)$	flow entering route $p \in P^{rs}$ during interval k
$\mathbf{f}$	vector of route flows $\left(f_p^{rs}(k), \forall r \in R, s \in S, p \in P^{rs}, k \in K_d\right)$
$d^{rs}(k)$	traffic demand of OD pair (r, s) during interval k
d^{rs}	traffic demand of OD pair (r, s)
$C_a(k)$	outflow capacity of link a during interval k
$t_a(k)$	link travel time for vehicles entering link $a \in A$ during interval k
$t_p^{rs}(k)$	route travel time for flow entering route $p \in P^{rs}$ during interval k
$c_p^{rs}(k)$	generalized route travel cost incurred by travelers entering route $p \in P^{rs}$ during interval k
$\overline{c}_p^{rs}(k)$	mean generalized route travel cost incurred by travelers entering route $p \in P^{rs}$ during interval k
$\overline{\mathbf{c}}$	vector of the mean generalized route travel costs $\left(\overline{c}_p^{rs}(k), \forall r \in R, s \in S, p \in P^{rs}, k \in K_d\right)$
$\mu_a(k)$	toll charge for vehicles entering link $a \in A$ during interval k
$\mu_p^{rs}(k)$	toll charge for vehicles entering route $p \in P^{rs}$ during interval k

$\underline{\omega}_p^{rs}(k)$ penalty cost of schedule delay early for vehicles entering route $p \in P^{rs}$ during interval k

$\bar{\omega}_p^{rs}(k)$ penalty cost of schedule delay late for vehicles entering route $p \in P^{rs}$ during interval k

$\bar{\eta}^{rs}(k)$ minimum mean generalized route travel cost for travelers between OD pair (r, s) departing during interval k

$\bar{\pi}^{rs}$ minimum mean generalized route travel cost between OD pair (r, s) during the studied period

Ω feasible solution set of the PDUO-SRDTC problem

Φ feasible solution set of the PDUO-RC problem

$U_a(k)$ cumulative flow entering link a by the end of interval k

$V_a(k)$ cumulative flow leaving link a by the end of interval k

$U_{ap}^{rs}(k)$ cumulative flow on route $p \in P^{rs}$ entering link a by the end of interval k

$V_{ap}^{rs}(k)$ cumulative flow on route $p \in P^{rs}$ leaving link a by the end of interval k

$M_p^{rs}(k)$ cumulative flow on route $p \in P^{rs}$ departing from origin r by the end of interval k

$N_p^{rs}(k)$ cumulative flow on route $p \in P^{rs}$ arriving at destination s by the end of interval k

2.2. Definition of network degradation

As shown in Fig. 1, a triangular fundamental diagram is assumed for the relationship between traffic flow q and density ρ on each link in the network. For a given link a, the fundamental diagram includes five parameters: a positive free-flow speed (v_a), a negative backward shockwave speed (w_a), a maximum flow or capacity (Q_a), a critical density (ρ_{crit}), and a jam density (ρ_{jam}). Any three of the five parameters can be used to determine the other two parameters.

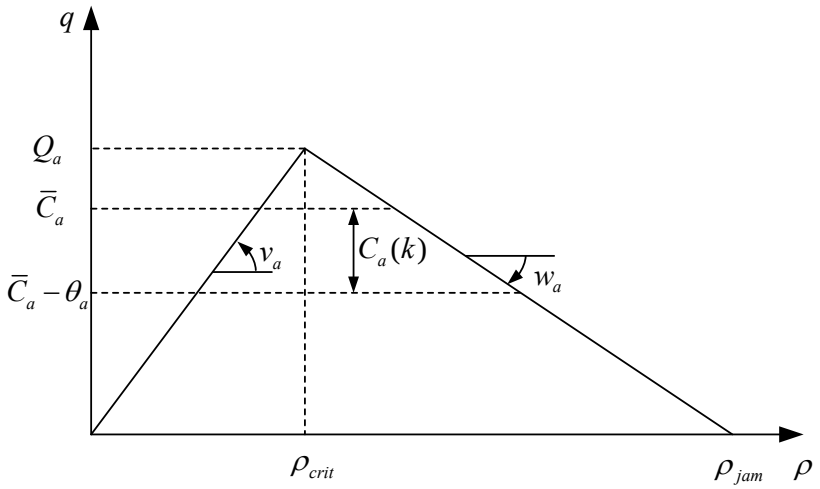

Fig. 1. A triangular fundamental diagram.

In a degradable road network, we assume that the capacity of each link is only degraded at the exit of the link due to stochastic vehicular interactions or incidents at intersections. Under this assumption, the outflow capacity of each link is a random variable subject to stochastic degradation, which adds variability to travelers' travel times. Without loss of generality, link outflow capacity follows a distribution with an upper bound (the

design outflow capacity) and a positive lower bound (the worst-degraded capacity). We also assume that link outflow capacity is time-varying and the outflow capacity of the same link during each interval follows the same distribution. Let $\bar{C}_a$ and θ_a be the design outflow capacity and the maximum degradation of the outflow capacity of link *a* (see Fig. 1). By definition, we have $C_a(k) \in [\bar{C}_a - \theta_a, \bar{C}_a]$. Let $g_a(C_a(k))$ and $G_a(C_a(k))$ be the probability density function and the cumulative distribution function of the link outflow capacity of link *a*, respectively.

2.3. Generalized route travel cost

We can obtain link cumulative flows and route cumulative flows from the procedure of DNL. Then, we can either directly retrieve route travel times from route cumulative flow curves (e.g., Lo and Szeto, 2002; Szeto and Lo, 2004, 2006; Long et al., 2013a) or indirectly deduce route travel times from link travel times that are derived from link cumulative flow curves (e.g., Long et al., 2011, 2015a). To explain the latter, we consider vehicles departing during time interval *k* and traveling through path $p = \{a_1, a_2, \cdots, a_m\}$. Their travel time on link a_1 is $t_{a_1}(k)$, and the time *instant* for leaving link a_1 and entering link a_2 is $k\delta + t_{a_1}(k) = k + t_{a_1}(k)$ (which may not be an integer). Then, their travel time on link a_2 is $t_{a_2}(k + t_{a_1}(k))$, and the time instant for leaving link a_2 and entering link a_3 is $k + t_{a_1}(k) + t_{a_2}(k + t_{a_1}(k))$. Similarly, we can obtain their travel times on other links. The route travel time of vehicles entering path $p \in P^{rs}$ during time interval *k* is equal to the sum of travel times on each link on that path, and can be computed by the following nested function:

$$t_p^{rs}(k) = t_{a_1}(k) + t_{a_2}(k + t_{a_1}(k)) + \cdots + t_{a_m}(k + t_{a_1} + \cdots + t_{a_{m-1}}), \quad (1)$$

where $t_{a_1} = t_{a_1}(k)$, $t_{a_2} = t_{a_2}(k + t_{a_1}(k))$, $\cdots$, for short. In Eq. (1), link travel times at both integer time instant and non-integer time instants are required to formulate path travel times. A linear interpolation procedure is applied to calculate the link travel times at non-integer time instants from link travel times at integer time instants. Link travel time at an integer time instant, which is numerically equivalent to link travel time associated with a particular time interval because δ = 1, can be obtained from link cumulative flow curves (e.g., Long et al., 2011, 2015a) by, for example, the step function (SF) approach (see Long et al, 2011 for details). If time is discretized, there is no guarantee that the traffic volume entering a link during a time interval will exit this link during the same time interval. For the SF-approach, the link travel time associated with a particular time interval is defined as the average link travel time of traffic volume entering the link during that interval.

In this paper, the generalized travel cost for travelers between OD pair (*r*, *s*) consists of four components: (1) the disutility of the trip travel time, (2) toll charge, (3) the penalty cost of schedule delay early, and (4) the penalty cost of schedule delay late. It is assumed that travelers have a common desired arrival time period, which is expressed as the arrival time window $[k_{rs}^* - \Delta_{rs}, k_{rs}^* + \Delta_{rs}]$, where k_{rs}^* is the middle point of the

time window and represents the official work start time for travelers between OD pair (*r*, *s*), and Δ_{rs} is the interval of arrival time flexibility. The generalized route travel cost for travelers departing from their origin *r* during time interval *k* and using path $p \in P^{rs}$ can be formulated as follows:

$$c_p^{rs}(k) = \alpha t_p^{rs}(k) + \mu_p^{rs}(k) + \underline{\omega}_p^{rs}(k) + \overline{\omega}_p^{rs}(k), \tag{2}$$

where

$$\underline{\omega}_p^{rs}(k) = \beta \cdot \max\{0, k_{rs}^* - \Delta_{rs} - k - t_p^{rs}(k)\}, \tag{3}$$

$$\overline{\omega}_p^{rs}(k) = \gamma \cdot \max\{0, k + t_p^{rs}(k) - k_{rs}^* - \Delta_{rs}\}, \tag{4}$$

α is the unit cost of travel time, and β and γ are the units cost of early and late arrivals, respectively.

The total toll charge to vehicles entering path $p \in P^{rs}$ during time interval *k* is equal to the sum of toll charges on each link on that path, and can be computed by the following nested function:

$$\mu_p^{rs}(k) = \mu_{a_1}(k) + \mu_{a_2}(k + t_{a_1}(k)) + \cdots + \mu_{a_m}(k + t_{a_1} + \cdots + t_{a_{m-1}}). \tag{5}$$

Similar to Eq. (1), a linear interpolation is required to determine link toll charges at non-integer time instants.

Because the outflow capacity of each link is a random variable subject to stochastic degradation, both link and route cumulative flows are stochastic variables. Link and route travel times are derived from the cumulative flow curves and hence are also stochastic variables. According to Eqs. (1)-(5), the generalized route travel costs are functions of link travel times, and hence are stochastic variables. By definition, the mean generalized route travel cost for travelers departing during time interval *k* and using path $p \in P^{rs}$ can be formulated as follows:

$$\overline{c}_p^{rs}(k) = E[c_p^{rs}(k)] = \alpha E[t_p^{rs}(k)] + E[\mu_p^{rs}(k)] + E[\underline{\omega}_p^{rs}(k)] + E[\omega_p^{rs}(k)]. \tag{6}$$

2.4. Probabilistic dynamic user optimal conditions

In this paper, we do not model the diversion or re-routing behavior in the event of a major incident. Instead, we aim to model the flow pattern after travelers acquire the expectation of route travel costs based on past experiences and settle into a long-term habitual equilibrium pattern. Therefore, the route flows associated with this long-term habitual equilibrium flow pattern are deterministic (Lo et al., 2006). We assume that commuters are aware of the degeneration probabilities of link design outflow capacities, and their route and departure time choice follows the UE principle in terms of the mean generalized route travel cost (Fosgerau, 2010; Xiao et al., 2015), i.e., commuters select routes and departure times to lower their own mean generalized route travel cost.

The ideal PDUO-SRDTC conditions can be stated as follows: For each OD pair, the mean generalized route travel costs incurred by travelers departing at any time are equal and minimal. The PDUO-SRDTC conditions require that for each route *p* between any OD pair (*r*, *s*), if route flow is positive during any

departure time interval k (i.e., $f_p^{rs}(k) > 0$), then the mean generalized route travel cost $\bar{c}_p^{rs}(k)$ must equal the minimal mean generalized route travel cost $\bar{\pi}^{rs}$. However, if the route flow is equal to zero (i.e., $f_p^{rs}(k) = 0$), then the corresponding mean generalized route travel cost $\bar{c}_p^{rs}(k)$ is at least equal to the minimal mean generalized route travel cost $\bar{\pi}^{rs}$.

The PDUO-SRDTC conditions can be written as follows:

$$\bar{c}_p^{rs}(k) \begin{cases} = \bar{\pi}^{rs}, \text{ if } f_p^{rs}(k) > 0, \\ \geq \bar{\pi}^{rs}, \text{ if } f_p^{rs}(k) = 0, \end{cases} \forall r \in R, s \in S, p \in P^{rs}, k \in K_d. \tag{7}$$

By definition, we have

$$\sum_{p \in P^{rs}} \sum_{k \in K_d} f_p^{rs}(k) = d^{rs}, \forall r \in R, s \in S, \text{ and} \tag{8}$$

$$f_p^{rs}(k) \geq 0, \forall r \in R, s \in S, p \in P^{rs}, k \in K_d. \tag{9}$$

Eq. (8) states that the total demand of an OD pair is equal to the sum of the corresponding route flows departing at any time interval. Constraint (9) states that route flows must be non-negative.

The feasible solution set of the PDUO-SRDTC problem can be expressed as follows:

$$\Omega = \left\{ \mathbf{f} \geq \mathbf{0} : \sum_{p \in P^{rs}} \sum_{k \in K_d} f_p^{rs}(k) = d^{rs}, \forall r \in R, s \in S \right\}. \tag{10}$$

2.5. Path-based VI formulation for the PDUO-SRDTC problem

The PDUO-SRDTC conditions (7) can be rewritten as a nonlinear complementarity problem (NCP) format, given by

$$\begin{cases} f_p^{rs}(k)[c_p^{rs}(k) - \bar{\pi}^{rs}] = 0, \forall r \in R, s \in S, p \in P^{rs}, k \in K_d, \\ c_p^{rs}(k) - \bar{\pi}^{rs} \geq 0, \forall r \in R, s \in S, p \in P^{rs}, k \in K_d, \\ f_p^{rs}(k) \geq 0, \forall r \in R, s \in S, p \in P^{rs}, k \in K_d. \end{cases} \tag{11}$$

The PDUO-SRDTC problem is to find $\mathbf{f} \in \Omega$ to satisfy condition (11) and can be reformulated as a VI problem as stated below:

Theorem 1. The PDUO-SRDTC conditions with fixed demand can be formulated as a finite-dimensional VI problem: find a vector $\mathbf{f}^* \in \Omega$ such that

$$\sum_{r \in R} \sum_{s \in S} \sum_{p \in P^{rs}} \sum_{k \in K_d} \bar{c}_p^{rs*}(k) \left[f_p^{rs}(k) - f_p^{rs*}(k) \right] \geq 0, \forall \mathbf{f} \in \Omega, \tag{12}$$

where $\mathbf{f}^* = \left(f_p^{rs*}(k), \forall r \in R, s \in S, p \in P^{rs}, k \in K_d \right)$.

The proof basically follows Theorem 2 in Friesz et al. (1993).

The VI problem (12) can be rewritten as the following VI problem: find a vector $\mathbf{f}^* \in \Omega$ such that

$$\left\langle \bar{\mathbf{c}}(\mathbf{f}^*), \mathbf{f} - \mathbf{f}^* \right\rangle \geq 0, \forall \mathbf{f} \in \Omega, \tag{13}$$

where $\overline{\mathbf{c}}(\mathbf{f}) = \left(\overline{c}_p^{rs}(k), \forall r \in R, s \in S, p \in P^{rs}, k \in K_d\right)$.

2.6. A special case of the PDUO-SRDTC problem: the PDUO-RC problem

If the departure time of travelers is fixed, we immediately obtain a special case of the PDUO-SRDTC problem: the PDUO-RC problem. If so, we have

$$\sum_{p \in P^{rs}} f_p^{rs}(k) = d^{rs}(k), \forall r \in R, s \in S. \tag{14}$$

The feasible solution set of the PDUO-RC problem with fixed demand can be expressed as follows:

$$\Phi = \left\{ \mathbf{f} \geq \mathbf{0} : \sum_{p \in P^{rs}} f_p^{rs}(k) = d^{rs}(k), \forall r \in R, s \in S, k \in K_d \right\}. \tag{15}$$

Similar to the PDUO conditions for the PDUO-SRDTC problems, the PDUO conditions for the PDUO-RC problems can be written as follows:

$$\overline{c}_p^{rs}(k) \begin{cases} = \overline{\eta}^{rs}(k), \text{ if } f_p^{rs}(k) > 0, \\ \geq \overline{\eta}^{rs}(k), \text{ if } f_p^{rs}(k) = 0, \end{cases} \forall r \in R, s \in S, p \in P^{rs}, k \in K_d. \tag{16}$$

Similar to the PDUO-SRDTC problem, the PDUO-RC problem can be formulated as a VI problem, which can be stated as follows:

Theorem 2. The PDUO-SRDTC conditions with fixed demand can be formulated as a finite-dimensional VI problem: find a vector $\mathbf{f}^* \in \Phi$ such that

$$\sum_{r \in R} \sum_{s \in S} \sum_{p \in P^{rs}} \sum_{k \in K_d} \overline{c}_p^{rs*}(k) \left[f_p^{rs}(k) - f_p^{rs*}(k) \right] \geq 0, \forall \mathbf{f} \in \Phi. \tag{17}$$

The VI problem (17) can be rewritten as the following VI problem: find a vector $\mathbf{f}^* \in \Phi$ such that

$$\left\langle \overline{\mathbf{c}}(\mathbf{f}^*), \mathbf{f} - \mathbf{f}^* \right\rangle \geq 0, \forall \mathbf{f} \in \Phi. \tag{18}$$

3. The Monte–Carlo-based stochastic link transmission model in a degradable network

The LTM can be considered a combination of Daganzo's (1995) CTM with a triangular fundamental diagram and Newell's (1993) solution scheme. Because each whole link is treated as one cell, the LTM's computational efficiency is much higher than that of classic numerical solution schemes for the LWR model, whilst retaining the same accuracy when the fundamental diagram is triangular. In this section, the MC-SLTM is developed to generate traffic states for DNL and collect travel time and travel cost statistics from each DNL. The DNL relies on a path-based LTM, which consists of a link model and a node model. The link model determines how flows travel through a link, while the node model determines how flows move from upstream links to downstream links.

3.1. Link model

In the link model, Newell's (1993) simplified theory of kinematic waves is used to determine the sending

and receiving flows. The sending flow of a link is constrained by both the boundary condition at the upstream end of the link and the outflow capacity of the link. According to Newell's (1993) simplified theory, if a free-flow traffic state occurs at the downstream end of the link at the end of interval *k*, then this state must have been emitted from the upstream end $\vec{\tau}_a = L_a / v_a$ time units earlier, where L_a is the length of link *a*, $\vec{\tau}_a$ is the free-flow travel time on link *a*. The sending flow of link *a*, $S_a(k)$, can be formulated as follows (Yperman, 2007):

$$S_a(k) = \min\{U_a(k+1-\vec{\tau}_a) - V_a(k), C_a(k)\}, \forall a \in A, k \in K . \tag{19}$$

The receiving flow of a link is constrained by both the boundary condition at the downstream end of the link and the inflow capacity of the link. If a congested traffic state occurs at the upstream end of the link at the end time of interval *k*, then this state must have been emitted from the downstream end of the link $\overleftarrow{\tau}_a = -L_a / w_a$ time units earlier, where $\overleftarrow{\tau}_a$ is the travel time required by the backward shockwave from the exit to the entry of link *a*. The receiving flow of link *a*, $R_a(k)$, can be formulated as follows (Yperman, 2007):

$$R_a(k) = \min\{V_a(k+1-\overleftarrow{\tau}_a) + L_a\rho_{jam} - U_a(k), Q_a\}, \forall a \in A, k \in K . \tag{20}$$

For each link, its inflow and outflow during interval *k* should be restricted by its sending and receiving flows during this interval. Hence, we have

$$U_a(k+1) - U_a(k) \le R_a(k), \forall a \in A, k \in K , \text{ and} \tag{21}$$

$$V_a(k+1) - V_a(k) \le S_a(k), \forall a \in A, k \in K . \tag{22}$$

3.2. Node model

The node model in the LTM is used to determine the transition flows from upstream links to downstream links, which rely on the sending and receiving flows belonging to all flow directions. We assume that the road traffic flows satisfy link first-in-first-out, i.e., vehicles that enter a link earlier will leave it sooner. According to this assumption, there exists an entry time instant λ_a^{k+1} by which all vehicles entering link *a* have left this link before the end of interval *k* + 1. Equivalently, we have $V_a(k+1) = U_a(\lambda_a^{k+1})$. Substituting this equation into inequality (21), and rearranging the resultant inequality, we have

$$U_a(\lambda_a^{k+1}) - V_a(k) \le R_a(k), \forall a \in A, k \in K . \tag{23}$$

Because the inflow capacity of each link is limited, a priority parameter $\vartheta_{ab}(k)$ is adopted to assign the receiving flow to each flow direction (Yperman, 2007; Long et al., 2015a), and hence we can obtain the receiving flow from link *a* to link *b* during interval *k*, i.e., $\vartheta_{ab}(k)R_b(k)$. The transition flow from an upstream link to a downstream link must be constrained by the sending flow of this direction, and hence we have

$$\sum_{r\in R}\sum_{s\in S}\sum_{p\in P^{rs}}\delta_{abp}^{rs}[V_{ap}^{rs}(k+1)-V_{ap}^{rs}(k)]\le \vartheta_{ab}(k)R_b(k), \tag{24}$$

where $\delta_{abp}^{rs}=1$ if link *b* is the next link after leaving link *a* along route *p* connecting OD pair (*r*, *s*); otherwise, $\delta_{abp}^{rs}=0$. The left-hand side of inequality (24) is the total flow leaving link *a* and entering link *b* during interval *k*.

By definition of λ_a^{k+1}, we have $V_{ap}^{rs}(k+1)=U_{ap}^{rs}(\lambda_a^{k+1})$. Substituting this equation into inequality (24), we have

$$\sum_{r\in R}\sum_{s\in S}\sum_{p\in P^{rs}}\delta_{abp}^{rs}[U_{ap}^{rs}(\lambda_a^{k+1})-V_{ap}^{rs}(k)]\le \vartheta_{ab}(k)R_b(k). \tag{25}$$

The node model aims to maximize the transition flow of each direction. The monotonically increasing property of the cumulative flows implies that the following one-dimensional optimization problem can be used to determine link enter time instant:

$$\begin{aligned}&\lambda_a^{k+1}=\max\lambda\\ &s.t.\begin{cases}U_a(\lambda)-V_a(k)\le R_a(k),\\ \sum_{r\in R}\sum_{s\in S}\sum_{p\in P^{rs}}\delta_{abp}^{rs}[U_{ap}^{rs}(\lambda)-V_{ap}^{rs}(k)]\le \vartheta_{ab}(k)R_b(k),\forall b\in\Gamma(h_a).\end{cases}\end{aligned} \tag{26}$$

We assume that vehicles from upstream links have a higher priority to enter downstream links than vehicles generated at the intersections of both upstream and downstream links and that the vehicles generated at the intersections (i.e., origins) can enter downstream links only if the capacities of downstream links are not fully used (Long et al., 2015a). The receiving flow of link *a* with respect to the corresponding origin *r* can be calculated by

$$R_a^r(k)=R_a(k)-\sum_{r\in R}\sum_{s\in S}\sum_{p\in P^{rs}}\sum_{b\in\Gamma^{-1}(r)}\delta_{bap}^{rs}[U_{bp}^{rs}(\lambda_b^{k+1})-V_{bp}^{rs}(k)]. \tag{27}$$

The second term on the right-hand side of Eq. (27) is the total number of vehicles that leave the upstream links of link *a* and enter link *a* during interval *k*.

Let $\lambda_a^{r,k+1}$ be the departure time instant before which all vehicles departing from origin *r* have entered link *a* by the end of interval *k* + 1. Similar to the determination of link entry time instant (λ_a^{k+1}), $\lambda_a^{r,k+1}$ can be expressed as follows:

$$\lambda_a^{r,k+1}=\max\left\{\lambda\left|\sum_{s\in S}\sum_{p\in P^{rs}}\delta_{ap}^{rs}\left[M_p^{rs}(\lambda)-U_{ap}^{rs}(k)\right]\le R_a^r(k)\right.\right\},\forall r\in R,a\in\Gamma(r),k\in K, \tag{28}$$

where $\delta_{ap}^{rs}=1$ if link *a* is the first link on route *p* connecting OD pair (*r*, *s*); otherwise, $\delta_{ap}^{rs}=0$. $M_p^{rs}(k)$ is the cumulative route flow on path $p\in P^{rs}$ by the end of interval *k*.

Using the link entry time instants and the departure time instants, we can update the cumulative flows as follows:

$$M_p^{rs}(k+1)=M_p^{rs}(k)+\delta f_p^{rs}(k),\forall r\in R,s\in S,p\in P^{rs},k\in K_d, \tag{29}$$

$$V_{ap}^{rs}(k+1) = U_{ap}^{rs}(\lambda_a^k), \forall a \in A, r \in R, s \in S, p \in P^{rs}, k \in K_d, \tag{30}$$

$$U_{ap}^{rs}(k+1) = \begin{cases} M_p^{rs}(\lambda_a^{r,k}), \text{ if } \delta_{ap}^{rs} = 1, \\ V_{bp}^{rs}(k+1), \text{ if } \delta_{bap}^{rs} = 1, \forall a \in A, r \in R, s \in S, p \in P^{rs}, k \in K_d, \\ 0, \text{ otherwise.} \end{cases} \tag{31}$$

$$N_p^{rs}(k+1) = \sum_{a \in A} \varsigma_{ap}^{rs} V_{ap}^{rs}(k+1), \forall r \in R, s \in S, p \in P^{rs}, k \in K_d, \tag{32}$$

$$V_a(k+1) = U_a(\lambda_a^k), \forall a \in A, k \in K, \text{ and} \tag{33}$$

$$U_a(k+1) = \sum_{r \in R} \sum_{s \in S} \sum_{p \in P^{rs}} U_{ap}^{rs}(k+1), \forall a \in A, k \in K. \tag{34}$$

where $\varsigma_{ap}^{rs} = 1$ if link *a* is the last link on route *p* connecting OD pair (*r*, *s*); otherwise, $\varsigma_{ap}^{rs} = 0$.

3.3. DNL for one realization in the MC-SLTM

The following procedure can be used to implement the path-based LTM for any given link outflow capacity vector $\mathbf{C} = [C_a(k)]$ and path flow vector $\mathbf{f}$ and to obtain the cumulative flow vectors $[U_a(k)]$, $[V_a(k)]$, $[U_{ap}^{rs}(k)]$, $[V_{ap}^{rs}(k)]$, $[M_p^{rs}(k)]$, and $[N_p^{rs}(k)]$:

Procedure 1: PATH_LTM ($\mathbf{C}$, $\mathbf{f}$)

Initialize all the cumulative flow vectors $[U_a(k)]$, $[V_a(k)]$, $[U_{ap}^{rs}(k)]$, $[V_{ap}^{rs}(k)]$, $[M_p^{rs}(k)]$, and $[N_p^{rs}(k)]$ to be zero, and set $k = 0$.

for each interval $k \in K$ **do**

  for each link $a \in A$ **do**

    Use Eqs. (19) and (20) to determine the sending flow $S_a(k)$ and the receiving flow $R_a(k)$.

    Solve problem (26) and obtain the entry time instant λ_a^k.

  end for

  for each origin $r \in R$ and $a \in A(r)$ **do**

    Obtain the departure time instant $\lambda_a^{r,k}$ by Eq. (28).

  end for

  Use Eqs. (29)-(34) to update cumulative flows by the end of interval *k*+1.

end for

Output the cumulative flow vectors $[U_a(k)]$, $[V_a(k)]$, $[U_{ap}^{rs}(k)]$, $[V_{ap}^{rs}(k)]$, $[M_p^{rs}(k)]$, and $[N_p^{rs}(k)]$.

The LTM is a physical queue model. In a physical-queue model, link inflow constraints, due to the physical lengths of vehicles and the storage capacity of each link, are considered (e.g., the receiving flow conditions in the LTM (Eq. (20))). If a physical queue uses up the storage capacity of a link (i.e., the queue fills up all the vacant spaces of a link), the queue passes over its upstream junction and spills back to its upstream links, and the inflow capacity of that link drops if the queue spills backward to the upstream boundary of that link. If link inflow constraints are omitted, the LTM immediately becomes a point queue model.

3.4. Evaluation of the mean generalized route travel cost

To obtain the mean generalized route travel costs, many realizations are generated by the MCS. To reduce computation time, the MC-SLTM incorporates the common random number MCS method and recursive formulas for determining mean route travel costs (Szeto et al., 2011; Meng and Liu, 2012; Liu and Meng, 2013). For given path flow vector $\mathbf{f}$ and sample size n, the following procedure will be adopted to compute the vector of mean generalized route travel costs $\bar{\mathbf{c}}(\mathbf{f}, n)$:

Procedure 2: MONTECARLO_ROUTECOST ($\mathbf{f}$, n)

Set $m = 1$.
while $m \le n$ **do**
  for each link $a \in A$ and interval $k \in K$ **do**
    Sample the link outflow capacity $C_a(k)^{(m)}$
  end for
  PATH_LTM ($\mathbf{C}^{(m)}$, $\mathbf{f}$)
  Update the route travel time vector $\mathbf{t}^{(m)}$ by using the cumulative route flow curves
  Update the generalized route travel cost vector $\mathbf{c}^{(m)}$ by Eq. (2)
  Estimate the mean generalized route travel cost vector $\bar{\mathbf{c}}^{(m)} = [(m-1)\mathbf{c}^{(m-1)} + \mathbf{c}^{(m)}]/m$
  $m = m + 1$
end do
Output the vector of mean generalized route travel costs $\bar{\mathbf{c}}(\mathbf{f}, n) = \bar{\mathbf{c}}^{(m)}$.

The inputs to Procedure 2 are the route flow vector $\mathbf{f}$ and the sample size n. In this procedure, firstly, the outflow capacity of each link during each time interval is sampled according to its distribution. Then, the sampled link outflow capacities and the path flow vector $\mathbf{f}$ are used as the inputs to Procedure 1 and run the path-based LTM. The cumulative route flow curves generated by Procedure 1 are then used to update the route travel time vector and the updated route travel time vector is further used to determine the generalized route travel cost vector and the mean generalized route travel cost vector. The above steps are repeated by n times and finally, the mean generalized route travel cost vector $\bar{\mathbf{c}}(\mathbf{f}, n)$ is outputted.

4. Solution algorithms

In this paper, the PDUO-SRDTC and PDUO-RC problems are formulated as VI problems, which can be solved by any general computational technique developed for VI problems, provided that the convergent requirements are satisfied. In this section, both the extragradient method (Long et al., 2013b, 2016b; Jiang et al., 2016) and the route swapping method (Huang and Lam, 2002; Szeto and Lo, 2006) are depicted and modified to solve the proposed DTA models.

4.1. Gap Functions

The convergence of the two algorithms is measured by gap function values. If the PDUO-SRDTC and PDUO-RC conditions are satisfied, the following two gap functions are respectively equal to zero:

$$G_1(\mathbf{f}) = \frac{\sum_{r\in R}\sum_{s\in S}\sum_{p\in P^{rs}}\sum_{k\in K_d}\delta f_p^{rs}(k)[\bar{c}_p^{rs}(k)-\bar{\pi}^{rs}]}{\sum_{r\in R}\sum_{s\in S}Q^{rs}\bar{\pi}^{rs}}, \text{ and} \tag{35}$$

$$G_2(\mathbf{f}) = \frac{\sum_{r\in R}\sum_{s\in S}\sum_{p\in P^{rs}}\sum_{k\in K_d}\delta f_p^{rs}(k)[\bar{c}_p^{rs}(k)-\bar{\pi}^{rs}(k)]}{\sum_{r\in R}\sum_{s\in S}\sum_{k\in K_d}q^{rs}(k)\bar{\pi}^{rs}(k)}. \tag{36}$$

If the PDUO-SRDTC (PDUO-RC) conditions are satisfied, then the numerator on the right-hand side of Eq. (35) (Eq. (36)) is equal to zero, and hence the gap function is also equal to zero. The denominator of the right-hand side of Eq. (35) (Eq. (36)) is the mean total system travel cost. Gap function (35) (Eq. (36)) is used to determine the relative gap of the current solution.

4.2. The modified extragradient method

The extragradient method was initially developed to solve VI problems (Korpelevich, 1976) and then was extended to solve static traffic assignment problems (e.g., Panicucci et al., 2007; Yook and Heaslip, 2016), DTA problems (e.g., Long et al., 2013b, 2016b; Jiang, et al., 2016), and transit assignment problems (e.g., Szeto and Jiang, 2014). The method has been shown to converge to an equilibrium flow if the route travel cost functions are pseudomonotone and Lipschitz continuous (Panicucci et al., 2007). Another merit of the extragradient method is that we do not need to know the Lipschitz constant of the path travel cost functions a priori.

In this paper, the mapping function of the proposed VI problems is the vector of mean generalized route travel costs, which is a function of the vector of route flows. The mean generalized route travel costs are estimated by the proposed MC-SLTM. In the proposed MC-SLTM, if more samples are used in procedure 2, the estimated mean generalized route travel costs will be more precise. However, it is time-consuming to implement procedure 2 when a large sample size is used. To overcome this limitation, we adopted variable sample sizes: small sample sizes were initially used and then increased according to the reduction of the relative gap. The following modified extragradient method can be adopted to solve VI problem (13):

Step 0. *Initialization*. Let $\mathbf{f}_1$ be any feasible route flow vector. Set the parameters ϑ, $\xi \in (0,1)$, $\bar{\lambda} > 0$, $\underline{\lambda} > 0$, the convergence tolerance $\varepsilon > 0$, the initial number of samples n_1, the increment of the sample size $\Delta n > 0$, and set $\lambda_1 = \bar{\lambda}$ and the iteration index $t = 1$.

Step 1. *Route flow update*.

Step 1.1. $\bar{\mathbf{f}}_t$ *computation*. Compute

$$\bar{\mathbf{f}}_t = \text{Proj}_{\Omega}(\mathbf{f}_t - \lambda_t \bar{\mathbf{c}}(\mathbf{f}_t, n_t)).$$

Step 1.2. *Stepsize determination*.

If $\lambda_t > \max\left\{\vartheta \frac{\left\|\mathbf{f}_t - \bar{\mathbf{f}}_t\right\|}{\left\|\bar{\mathbf{c}}(\mathbf{f}_t, n_t) - \bar{\mathbf{c}}(\bar{\mathbf{f}}_t, n_t)\right\|}, \underline{\lambda}\right\}$, then reduce λ_t using

$$\lambda_t = \min\left\{\xi\lambda_t, \vartheta \frac{\left\|\mathbf{f}_t - \bar{\mathbf{f}}_t\right\|}{\left\|\bar{\mathbf{c}}(\mathbf{f}_t, n_t) - \bar{\mathbf{c}}(\bar{\mathbf{f}}_t, n_t)\right\|}\right\},$$

and return to Step 1.1.

Step 1.3. *Computation of* $\mathbf{f}_{t+1}$ *and* λ_{t+1}. Update the route flow vector by

$\mathbf{f}_{t+1} = \text{Proj}_{\Omega}(\mathbf{f}_t - \lambda_t \bar{\mathbf{c}}(\bar{\mathbf{f}}_t, n_t))$ and

set $\lambda_{t+1} = \min\left\{\bar{\lambda}, \vartheta \frac{\left\|\mathbf{f}_t - \bar{\mathbf{f}}_t\right\|}{\left\|\bar{\mathbf{c}}(\mathbf{f}_t, n_t) - \bar{\mathbf{c}}(\bar{\mathbf{f}}_t, n_t)\right\|}\right\}$.

Step 2. *Convergence criterion*. Terminate the algorithm if $G_1(\mathbf{f}_{t+1}) < \varepsilon$.

Step 3. *A sample size increase*. If $G_1(\mathbf{f}_{t+1}, n_{t+1}) > G_1(\mathbf{f}_t, n_t)$, then $n_{t+1} = n_t + \Delta n$; otherwise, $n_{t+1} = n_t$. Set $t = t+1$ and return to Step 1.

In Step 0, an all-or-nothing assignment under the free-flow condition can be used to determine the feasible route flow vector $\mathbf{f}_1$. In Step 1, $\text{Proj}_{\Omega}(\mathbf{f})$ is the Euclidean projection map onto Ω. $\mathbf{f}_t$, n_t, and λ_t are the route flow vector, the sample size, and the step size at iteration t, respectively. Because the mapping function of VI problem (13) may not be pseudomonotone, a minimum step size $\underline{\lambda}$ was used in Step 1.2 to avoid slow convergence due to small step sizes. A re-initialization of the step size was used in Step 1.3 to avoid the problem of the reduction of the convergence rate due to excessively small step sizes at some iterations. In Step 3, the sample size is enlarged if the relative gap cannot be reduced. We note that the extragradient method may be considered a heuristic because the required conditions (such as pseudomonontonicity) may not be satisfied.

The proposed extragradient method can also be directly extended to solve VI problem (18), provided that the convergence requirement is satisfied. If the proposed extragradient method is applied to solve the PDUO-RC problem, we need only replace the feasible solution set Ω by Φ, and change the gap function $G_1(\mathbf{f}_t)$ by $G_2(\mathbf{f}_t)$.

4.3. The modified route-swapping method

The day-to-day route-swapping algorithm has been widely used to solve static traffic assignment problems (e.g., Smith, 1984; Jin, 2007; Bie and Lo, 2010) and DTA problems (Huang and Lam, 2002; Szeto and Lo, 2006; Tian et al., 2012; Long et al., 2016b). The convergence of the route-swapping algorithm is guaranteed if

the mapping function is continuous and monotone (Mounce and Carey, 2011). The numerical results presented in Long et al. (2016b) show that the route-swapping method outperforms the extragradient method in terms of solving the DUO-SRDTC problems. In this paper, we extended the route-swapping method proposed by Huang and Lam (2002) to solve the proposed PDUO-SRDTC problem. The detailed algorithm is given as follows:

Step 1. *Initialization*. Choose an initial vector of route flows $\mathbf{f}_1$, the convergence tolerance $\varepsilon > 0$, the initial number of samples n_1, the increment of the sample size $\Delta n > 0$, and the iteration index $\iota = 1$.

Step 2. *Calculation of mean generalized route travel costs*. Implement Procedure 2 to estimate the vector of the mean generalized route travel costs $\bar{\mathbf{c}}(\mathbf{f}_\iota, n_\iota)$. Obtain the minimum mean generalized route travel cost for each OD pair and the corresponding path set of each OD pair, respectively, by

$$\pi_\iota^{rs} = \min\{c_p^{rs}(k)_\iota : p \in P^{rs}, k \in K_d\}, \forall r \in R, s \in S, \text{ and} \tag{37}$$

$$\hat{P}_\iota^{rs} = \min\{(p,k) : c_p^{rs}(k)_\iota = \bar{\pi}_\iota^{rs}, p \in P^{rs}, k \in K_d\}, \forall r \in R, s \in S. \tag{38}$$

Step 3. *Route flow update*. Calculate the route flow vector $\mathbf{f}_{\iota+1}$ by

$$f_p^{rs}(k)_{\iota+1} = f_p^{rs}(k)_\iota - \lambda_\iota f_p^{rs}(k)_\iota [\bar{c}_p^{rs}(k)_\iota - \pi^{rs}{}_\iota], \forall r \in R, s \in S, p \in P^{rs}, k \in K_d, \text{ and} \tag{39}$$

$$f_p^{rs}(k)_{\iota+1} = f_p^{rs}(k)_\iota + \frac{\psi_\iota^{rs}}{|\hat{P}_\iota^{rs}|}, \forall (p,k) \in \hat{P}_\iota^{rs}, \forall r \in R, s \in S, \tag{40}$$

where

$$\psi_\iota^{rs} = \sum_{p \in P^{rs}} \sum_{k \in K_d} \rho_\iota f_p^{rs}(k)_\iota [\bar{c}_p^{rs}(k)_\iota - \bar{\pi}_\iota^{rs}], \forall r \in R, s \in S.$$

Step 4. *Convergence criterion*. If $G_1(\mathbf{f}_\iota) < \varepsilon$, then stop the algorithm; otherwise, set $\iota = \iota + 1$, $n_\iota = n_{\iota-1} + \Delta n$, and go to Step 2.

In Step 0, an all-or-nothing assignment under the free-flow condition can also be used to determine the feasible route flow vector $\mathbf{f}_1$. In Eq. (39), λ_ι is the step size at the ιth iteration. Because the performance of the step-size sequence depicted in Tian et al. (2012) was better than that depicted in Huang and Lam (2002), we adopted the following step-size method to calculate the step size in Step 3 (Tian et al., 2012):

$$\lambda_\iota = 0.012\{1^{(1\to1000)}, 1/2^{(1001\to2000)}, 1/3^{(2001\to3000)}, \cdots\}. \tag{41}$$

The above route-swapping method can also be directly extended to solve the PDUO-RC problem, provided that the convergence requirement is satisfied. However, the route-swapping method is inferior to the extragradient method in terms of solving the PDUO-RC problem. Hence, the description of the route-swapping method for the PDUO-RC problem is omitted here.

5. Numerical examples

In this section, six experiments were conducted to illustrate paradoxical phenomena and the performance of the proposed algorithms. All experiments were run on a computer with an Intel (R) Core(TM) 2 Quad Q9550 2.83GHz CPU and a 3.5GB RAM.

For all experiments, the uniform distribution was used for link outflow capacities. By definition, the average outflow capacity of a given link a is $C_a - \theta_a/2$. The networks were empty initially and no toll was charged on each link. The value of time and the unit costs of schedule delay were set as follows: α = 10 \$/h, β = 4 \$/h, and γ = 20 \$/h (Qian et al., 2012). The PDUO-RC and PDUO-SRDTC problems were solved by the proposed extragradient method and route-swapping method, respectively. The values of the parameters for the extragradient method were $\vartheta = 0.8$, $\xi = 0.9$, and $\bar{\lambda} = 10.0$. Unless otherwise specified, the parameters related to the sample size were $n_1 = \Delta n = 10$ and the convergence tolerance $\varepsilon = 1.0 \times 10^{-2}$. The SF-type route travel time model proposed by Long et al. (2013a) was adopted to calculate route travel times. Unless specified otherwise, the input parameters of the MC-SLTM for each link in all example networks were the same and are given as follows:

- Jam density: 133 vehicles/km (i.e., 7.5 m for every vehicle).
- Free-flow speed: 54 km/h (i.e., 15 m/s), and backward shockwave speed: -18 km/h (i.e., -5 m/s).
- Flow capacity: 1800 vehicles/h/lane (i.e., 0.5 veh/s/lane).
- Length of each time interval δ: 10 s.

As mentioned before, the PDUO-RC problem is a special case of the PDUO-SRDTC problem in which travelers' departure times are fixed. This implies that the conclusions of the PDUO-RC problem can be generalized to the PDUO-SRDTC problem. Compared with the PDUO-SRDTC problem, the PDUO-RC problems is easier to be solved, and the examples constructed by the PDUO-RC problem can be followed more easily and can illustrate the paradoxical phenomena more clearly. Therefore, we mainly used the PDUO-RC problem to illustrate paradoxical phenomena in degradable networks (see Examples 1-3 for details) and developed Example 4 to verify that the conclusions of the PDUO-RC problem can be generalized to the PDUO-SRDTC problem. Examples 5 and 6 are given to illustrate the convergence of the modified extragradient method and the modified route swapping method, respectively. Example 5 also demonstrates the effectiveness of the variable sample size scheme.

Example 1: The addition of a link may result in an increase in TSTC due to network degradation and queue spillback.

This example adopted two test networks as shown in Fig. 2. Fig. 2(a) shows the network before a new link was constructed. This network had six nodes, five links, and two OD pairs (i.e., OD pairs (1, 3) and (2, 4)). Each OD pair was connected by a single path. Fig. 2(b) reveals the network after link 2-5 was constructed to connect node 2 and node 5. After adding link 2-5, OD pair (2, 4) had a new path 2-5-6-4. The design outflow capacities were 15 veh/interval for link 1-5, 5 veh/interval for link 5-6, and 10 veh/interval for other four links. The maximum degradations of outflow capacities were 1 veh/interval for all links except link 1-5, whose

maximum degradation were varied for the purpose of conducting sensitivity analysis. A traffic signal was located at the exit of link 6-4, with a cycle time of 16 intervals and a green time of eight intervals. The green time started at the ninth interval and the upper bound of the outflow capacity of link 6-4 was 10 veh/interval during the green phase. The free-flow speed and backward shockwave speed were respectively 7.5 m/s and -7.5m/s for link 6-4. The free-flow travel times were 2 intervals for link 2-5 and 1 interval for other five links. In this example, only the PDUO-RC problem for each test network was considered and the penalty costs of schedule delay early and late were ignored. The OD demand rates of OD pairs (1, 3) and (2, 4) were both 20 veh/interval and lasted for the first 5 and 3 intervals, respectively. Note that due to degradable link outflow capacities and link inflow capacities, the demand of each OD pair may not be able to flow into a test network and queue and wait at the origin node.

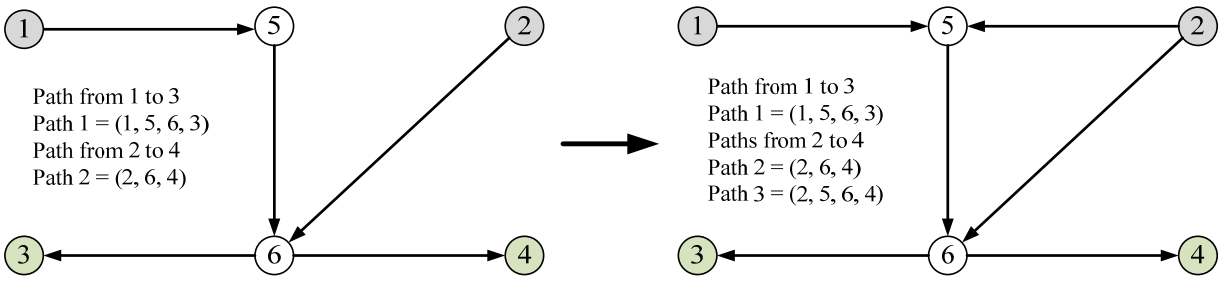

(a) Before the addition of link 2-5 (b) After the addition of link 2-5

Fig. 2. The test networks for Example 1.

In both test networks, OD pair (1, 3) was connected by a single path (i.e., path 1: 1-5-6-3). This path had three links, in which link 5-6 had the smallest average outflow capacity. Hence, link 5-6 was the key bottleneck of this path. Before adding link 2-5, OD pair (2, 4) was also connected by a single path (i.e., path 2: 2-6-4). This path had two links, which had the same design outflow capacity and maximum degradation of outflow capacity. However, the signal on link 6-4 was in the red phase during the first eight time intervals, and this link was the key bottleneck of this path. Path 1 and path 2 were separate (due to junction design at node 6), and hence the traffic flow along the two paths had no interaction. After adding link 2-5, there was a new path (i.e., path 3: 2-5-6-4) connecting OD pair (2, 4). Link 5-6 was the single common link of both path 1 and path 3. The traffic flow that traveled through path 3 must use some outflow capacity of link 5-6. Therefore, when path 3 carried some flow, the capacity of link 5-6 available for the traffic flow of OD pair (1, 3) was smaller compared with the case that path 3 carried no flow. As a result, traffic flow from origin 1 spent more travel time to destination 3 and had a larger travel cost when path 3 carried some flow. Meanwhile, some traffic flow of OD pair (2, 4) whose used path 3 did not change the travel time and travel cost between OD pair (2, 4), because link 6-4 was the single common link of both path 2 and path 3 between OD pair (2, 4) and was the key bottleneck of this OD pair (i.e., the travel time between OD pair (2, 4) was mainly restricted by the average capacity of this link). Therefore, the network with link 2-5 had a higher TSTC than the network without link 2-5 if the traffic flow on path 3 was positive.

We varied the maximum degradation of the outflow capacity of link 1-5 (i.e., $\theta_{1\text{-}5}$) for the networks with and without link addition, solved the corresponding PDUO-RC problem, and computed the corresponding TSTC (see Fig. 3(a)) and the total traffic flow on path 3 (see Fig. 3(b)). We can observe from the black lines of these figures that the total traffic flow on path 3 and the increase in TSTC after adding link 2-5 are equal to zero when $\theta_{1\text{-}5} \le 7.0$ veh/interval, and are positive when $\theta_{1\text{-}5} > 7.0$ veh/interval. This result is consistent with our previous analysis that the presence of traffic flow on path 3 (which occurred when $\theta_{1\text{-}5} > 7.0$ veh/interval) can increase the travel cost of traffic flow from origin 1 to destination 3 and can lead to a larger TSTC compared with the case that path 3 carried no flow. The result also indicates that the addition of a link to a network can lead to a decrease in network performance in terms of TSTC when the degradation is large enough. Moreover, these figures show that as $\theta_{1\text{-}5}$ gets larger, more traffic flow is on path 3 and the percentage increase in TSTT is larger. This is because when $\theta_{1\text{-}5}$ gets larger, because less flow from node 1 could use the capacity of link 5-6 and more capacity could be allocated to path 3 and hence path 3 was more attractive and more flow generated at node 2 was attracted to path 3, allowing the flow arriving at node 6 earlier. Moreover, when $\theta_{1\text{-}5}$ gets larger, the travel cost of traffic flow from origin 1 to destination 3 is larger and the travel time between OD pair (2, 4) remained unchanged (as explained earlier), and hence the TSTC are larger.

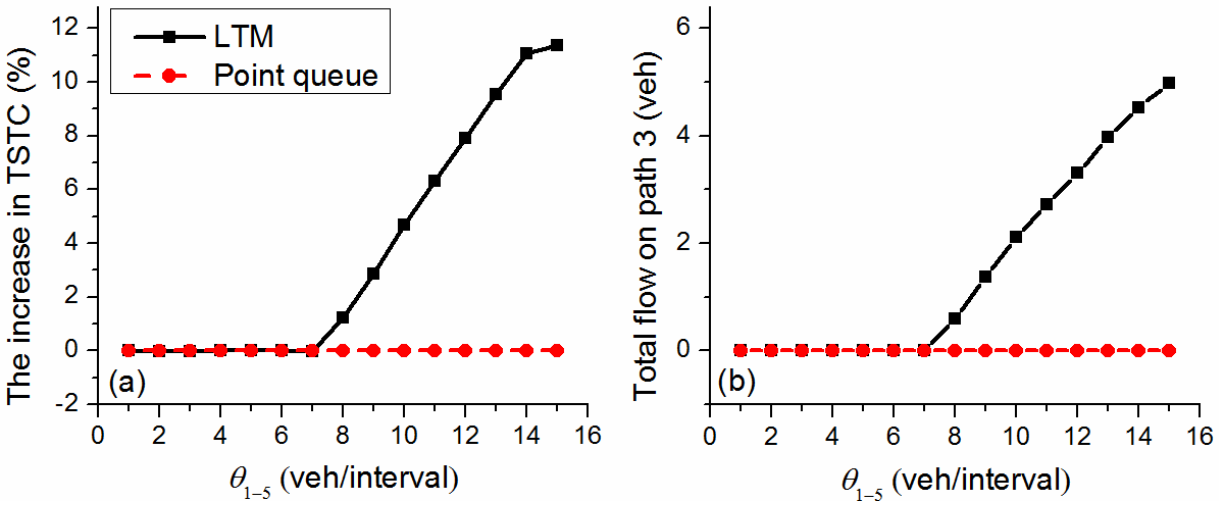

(a) The percentage increase in TSTC (b) The total flow on path 3

Fig. 3. The increase in TSTC and the total flow on path 3 after the addition of link 2-5.

To illustrate the occurrence of queue spillback, we set the maximum degradation of the outflow capacity of link 1-5 to be 10 veh/interval and solved the corresponding PDUO-RC problem for each test network. Fig. 4 illustrates the average outflows of links 2-6, 5-6, and 6-4 under the PDUO-RC conditions. We can see that the outflows of links 2-6 and 5-6 have a drop since the fifth and eighth intervals, respectively, due to queue spillback from link 6-4.

If we set the inflow capacities and the maximum occupancies of all links to be infinite, the LTM immediately becomes a point queue model. Using the point queue model, we repeated the experiment and computed the TSTC. The increase in TSTC and the total traffic flow on path 3 are graphically shown in Fig. 3(a) and (b), respectively. We can observe that no traffic flows are on path 3 and the increase in TSTC is zero as the value of $\theta_{1\text{-}5}$ increases. This implies that the paradox did not occur when a point queue model was used as the DNL model. In addition, we also considered that the two networks were not degradable. We solved the PDUO-RC problems for both networks without degradation and found that the TSTCs were both \$45. This implies that the addition of link 2-5 to the network in Fig. 2(a) did not lead to an increase in TSTC if the two networks were not degradable. In summary, a paradox may occur only when the test networks in Fig. 2 are degradable and the physical queue model is considered.

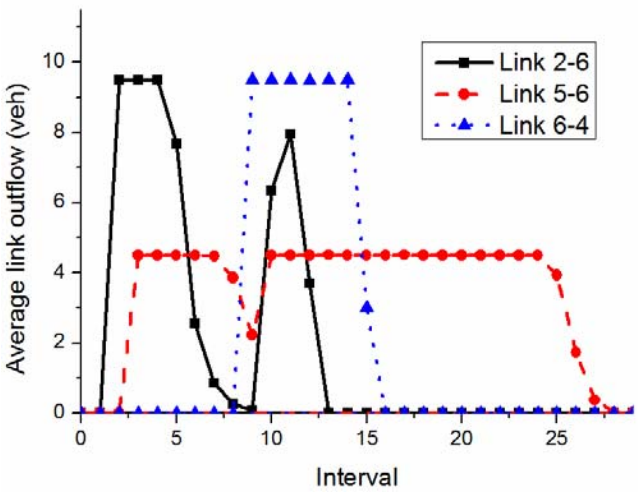

Fig. 4. Average link outflow under the PDUO-RC conditions ($\theta_{1\text{-}5} = 10$ veh/interval).

Example 2: An improvement of road design outflow capacity may result in an increase in TSTC due to network degradation and queue spillback.

This example adopted the test network as shown in Fig. 5. This network had seven nodes, seven links, and three OD pairs (i.e., OD pairs (1, 5), (2, 3), and (2, 4)). The design outflow capacities were 15 veh/interval for link 1-6, 5 veh/interval for link 6-7, and 10 veh/interval for other five links. The maximum degradations of outflow capacities were 10 veh/interval for link 1-6 and 1 veh/interval for other six links. A traffic signal was located at the exit of link 7-4, with a cycle time of 16 intervals and a green time of eight intervals. The green time started at the ninth interval, and the upper bound of the outflow capacity of link 7-4 was 10 veh/interval during the green phase. The free-flow speed and backward shockwave speed were respectively 7.5 m/s and -7.5 m/s for link 7-4. The free-flow travel times were 2 intervals for link 2-6 and 1 interval for other six links. In this example, only the PDUO-RC problem was considered and the penalty costs of schedule delay early and late were ignored. The OD demand rates of OD pairs (1, 5), (2, 3), and (2, 4) were 20 veh/interval, 10 veh/interval, and 20 veh/interval, and lasted for the first 5, 4, and 3 intervals, respectively.

In this test network, OD pairs (1, 5) and (2, 3) were connected by a single path (i.e., path 1: 1-6-7-5, and path 2: 2-6-3, respectively). Path 1 had three links, in which link 6-7 had the smallest average outflow capacity and was the key bottleneck of this path. Path 2 had two links, in which link 6-3 had the smallest average outflow capacity and was the key bottleneck of this path. OD pair (2, 4) was connected by two paths (i.e., path 3: 2-6-7-4 and path 4: 2-7-4). Link 7-4 was the single common link of paths 3 and 4. Due to the red phase of the signal at the exit of link 7-4, the traffic flow of OD pair (2, 4) was mainly restricted by the outflow capacity of this link. Meanwhile, the traffic flow that traveled through path 3 must use some outflow capacity of link 6-7. Consequently, a smaller capacity of link 6-7 was available for the traffic flow between OD pair (1, 5) when the flow on path 3 was larger. As a result, traffic flow from origin 1 spent more travel time to destination 5 and had a larger travel cost if the traffic flow on path 3 was larger. On the other hand, compared with no flow on path 3, having traffic flow on path 3 could not reduce the total travel time and total travel cost of traffic flow belonging to OD pair (2, 3) as there was only one path between this OD pair. For OD pair (2, 4), having traffic flow on path 3 did not change the OD travel time and the total travel cost of the traffic flow of that OD pair compared with no flow on path 3. This was because link 7-4 was the key bottleneck for traffic flow belonging to OD pair (2, 4), respectively.

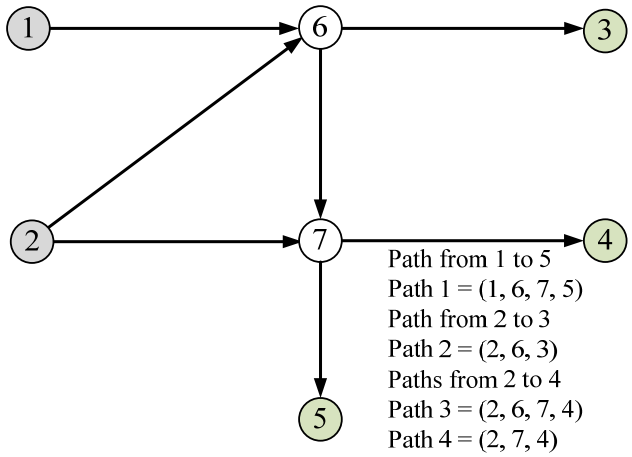

Fig. 5. The test network for Examples 2 and 3.

We varied the design outflow capacity of link 2-6, solved the corresponding PDUO-RC problem, and computed the corresponding TSTC (see Fig. 6). We can see from the red line that the TSTC initially decreases until the design outflow capacity of link 2-6 equals 9 veh/interval. This is because the design outflow capacity of link 6-3 was 10 veh/interval, the bottleneck of path 2 (2-6-3) was on link 2-6 and a larger design outflow capacity of link 2-6 could provide a higher capacity for traffic flow belonging to OD pair (2, 3), leading to a lower travel time on that link and the travel time between OD pair (2, 3). Moreover, when the design outflow capacity of link 2-6 was less than 9 veh/interval, no traffic flow of OD pair (2, 4) used path 3 (2-6-7-4) and the travel time between OD pair (2, 4) was unchanged. However, we can observe from Fig. 6 that the TSTC increases as the design outflow capacity of link 2-6 increases from 9 to 12 veh/interval. In this range of

outflow capacity, although the travel time on link 2-6 decreased with an increasing design outflow capacity of link 2-6, some traffic flow of OD pair (2, 4) was attracted to use path 3 (2-6-7-4), leading to the occurrence of queue spillback from link 7-4 to link 6-7. As a result, the travel costs between OD pair (1, 5) in the range of design outflow capacity considered were much higher than those in the range from 0 to 9 veh/interval. Moreover, the more the flow attracted to use path 3, the more serious the queue spillback occurred, and the higher the travel cost between OD pair (1, 5) was. Therefore, the TSTC increased as the design outflow capacity of link 2-6 increased from 9 to 12 veh/interval. When the design outflow capacity of link 2-6 was greater than 12 veh/interval, the inflow rate of link 2-6 was always not greater than 12 veh/interval and the traffic flow on link 2-6 was always under the free flow condition. Therefore, the TSTC was unchanged when the design outflow capacity of link 2-6 was larger than 12 veh/interval. In summary, the result presented in Fig. 6 indicates that an improvement of road design outflow capacity may result in an increase in TSTC when the network is degradable.

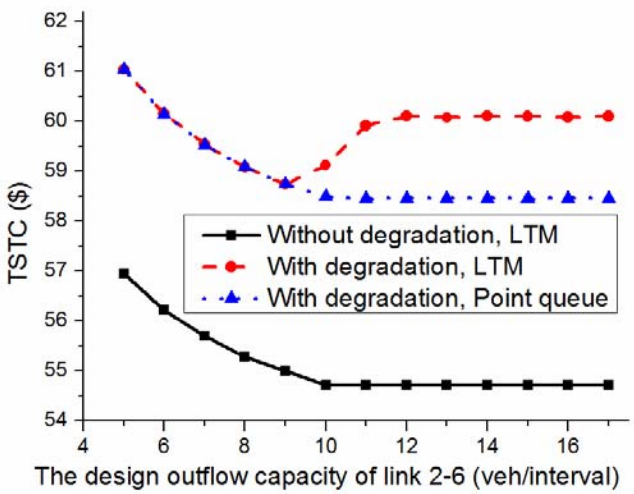

Fig. 6. The influence of the design outflow capacity of link 2-6 on TSTC.

We also considered that the test network was not degradable. We varied the design outflow capacity of link 2-6, solved the corresponding PDUO-RC problem, and computed the corresponding TSTC (see the black line of Fig. 6). We can observe from Fig. 6 that the TSTC drops when the design outflow capacity of link 2-6 is less than or equal to 10 veh/interval. This is similar to the observation in the decreasing range for the network with degradation. One difference is that for the same design outflow capacity of link 2-6, the TSTC for the degradable network is larger than that of the non-degradable network as the expected network capacity for the former is smaller. Another difference is that the decreasing range for the non-degradable network is slightly larger than that for the degradable network. The main reasons are that the deterministic outflow capacity of link 6-3 is 10 veh/interval and no queue spilled back from 7-4 to link 6-7 in the range of the design outflow capacity of link 2-6 considered. As the design outflow capacity of link 2-6 was less than that of link 6-3 (which was 10 veh/interval), the traffic flow of OD pair (2, 3) was restricted by the outflow capacity of

link 2-6 and therefore increasing the design outflow capacity of link 2-6 could improve the TSTC and the maximum design outflow capacity could be up to 10 veh/interval. Moreover, both links 2-7 and 7-4 in a nondegradable network had a larger outflow capacity and the traffic flow on path 4 had less travel time and travel cost than those in the degradable network. Therefore, when the test network was not degradable, no traffic flow of OD pair (2, 4) used path 3, and hence no queue spilled back from 7-4 to link 6-7. However, as shown in Fig. 6, the TSTC no longer decreases but remains unchanged when the design outflow capacity of link 2-6 is larger than 10 veh/interval as the design outflow capacity of link 6-3 restricted the traffic flow of OD pair (2, 3).

We also adopted the point queue model as the DNL model, repeated the analysis, and plotted the result in Fig. 6. We can observe the blue line from Fig. 6 that the TSTC monotonically decreases as the design outflow capacity of link 2-6 increases. This implies that an improvement of design outflow capacity does not lead to a worse network performance in terms of TSTC than the do-nothing case when the effect of physical queues is not considered.

In summary, a paradox may occur only when the test network in Fig. 5 is degradable and the physical queue model is considered.

Example 3: An increase in the maximum degradation of outflow capacity may result in a decrease in TSTC.

This example also adopted the same test network as that in Example 2. In this example, we only changed the design outflow capacity of link 6-3 to be 5 veh/interval and the maximum degradation of the outflow capacity of link 1-6 to be 10 veh/interval. All other parameters are the same as those in Example 2. We varied the maximum degradation of the outflow capacity of link 2-6, solved the corresponding PDUO-RC problem, and computed the corresponding TSTC (see Fig. 7). We can observe that the TSTC may decrease as the maximum degradation of the outflow capacity of link 2-6 increases. This implies that increasing network uncertainty can lead to an improvement of network performance in terms of TSTC.

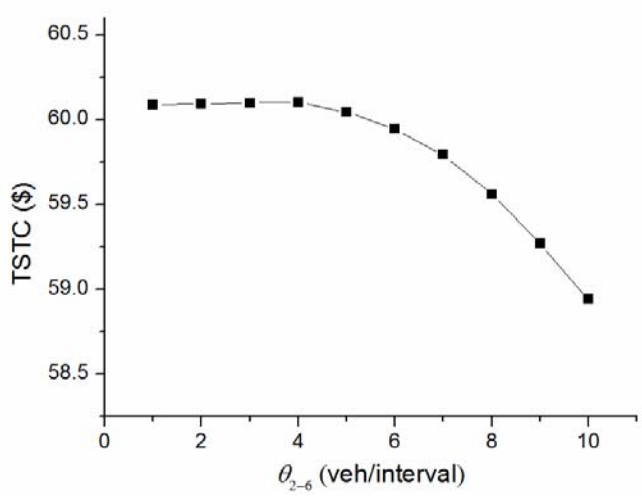

Fig. 7. The influence of the maximum degradation of the outflow capacity of link 2-6 on TSTC.

Example 4: The addition of a link may result in an increase in TSTC under the PDUO-SRDTC conditions.

This example adopted two test networks as shown in Fig. 8. Fig. 8(a) shows the network before a new link was constructed. This network had five nodes, four links, and two OD pairs (i.e., OD pairs (1, 2) and (1, 3)). Each OD pair was connected by a single path. Fig. 8(b) reveals the network after link 4-5 was constructed to connect Node 4 and Node 5. After adding link 4-5, OD pair (1, 3) had a new path 1-4-5-3. The design outflow capacities were 18 veh/interval for link 1-5 and 20 veh/interval for other links. The maximum degradations of outflow capacities were 1 veh/interval for links 1-4, 4-2, and 4-5, and 5 veh/interval for link 5-3. The free-flow travel times were one interval for all links. The total OD demands of both OD pairs (1, 2) and (1, 3) were 85 veh. The parameters for the arrival time window were k_{rs}^{*} = 12 intervals and Δ_{rs} = 0 interval. In the test networks, the storage capacity is very large so that no spillback occurred, and we adopted the route travel time model proposed by Huang and Lam (2002) to calculate route travel times.

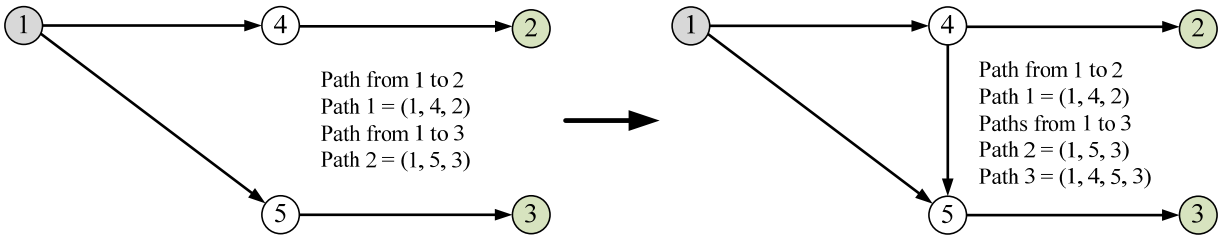

(a) Before the addition of link 4-5 **(b)** After the addition of link 4-5

Fig. 8. The test network for Examples 4 and 6.

We varied the maximum degradation of the outflow capacity of link 1-5 (i.e., $\theta_{1\text{-}5}$) for the networks with and without link addition, solved the corresponding PDUO-SRDTC problem, and computed the corresponding TSTC (see Fig. 9). The result clearly indicates that the addition of a link to a network can lead to a decrease in network performance in terms of TSTC under the PDUO-SRDTC conditions. In particular, we can observe from Fig. 9 that both the total traffic flow on path 3 and the increase in TSTC after adding link 4-5 are equal to zero when $\theta_{1\text{-}5} \le 7.0$ veh/interval, and are positive when $\theta_{1\text{-}5} > 7.0$ veh/interval. The reason is as follows. Path 3 (1-4-5-3) could only be attractive to the traffic flow between OD pair (1, 3) and carried flow when the non-overlapping link on the alternative path (path 2) could be seriously degraded (i.e., $\theta_{1\text{-}5} > 7.0$ veh/interval). When path 3 carried flow, the travel cost between OD pair (1, 2) was higher than that when path 3 carried no flow, because the total traffic flow and travel time on link 1-4 were larger. Although the travel cost between OD pair (1, 3) was lower, the increase in the total travel cost of the traffic flow of that OD pair (1, 2) is larger than the reduction of the total travel cost of travel flow of OD pair (1, 3), leading to a larger TSTC after adding link 4-5. Therefore, when link 1-5 was seriously degraded, both the total traffic flow on path 3 and the increase in TSTC after adding link 4-5 are positive; otherwise, path 3 was not

used and they were both equal to zero.

Example 5: A test on the convergence of the modified extragradient method for the PDUO-RC problem using the Nguyen and Dupius network and different sample size schemes.

We adopted the Nguyen and Dupius network (see Fig. 10) to illustrate the performance of the proposed algorithm. The network had 13 nodes, 19 links, and 4 OD pairs. The length of each link is given in Table 1. The modeling horizon was set to be 200 intervals, and each of the OD demand rates lasted for the first 10 intervals. The OD demand rates were 7.5 veh/interval for OD pair (1, 2), 15 veh/interval for OD pair (1, 3), and 10 veh/interval for OD pairs (4, 2) and (4, 3). The numbers of lanes were 1 for links 8-2, 12-8, and 13-3, 2 for links 7-8 and 9-13, and 3 for other 14 links. The design outflow capacities of links heading to nodes 2, 3, 5, 6, 9, 10, and 11 were 2.5 veh/interval/lane.

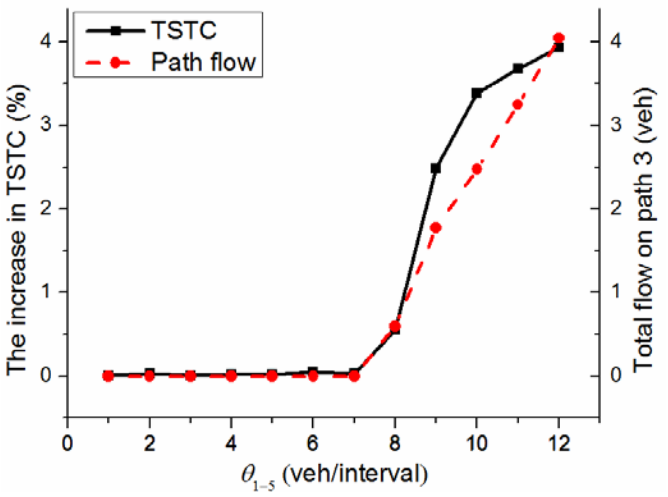

Fig. 9. The increase in TSTC and the total flow on path 3 after the addition of link 4-5.

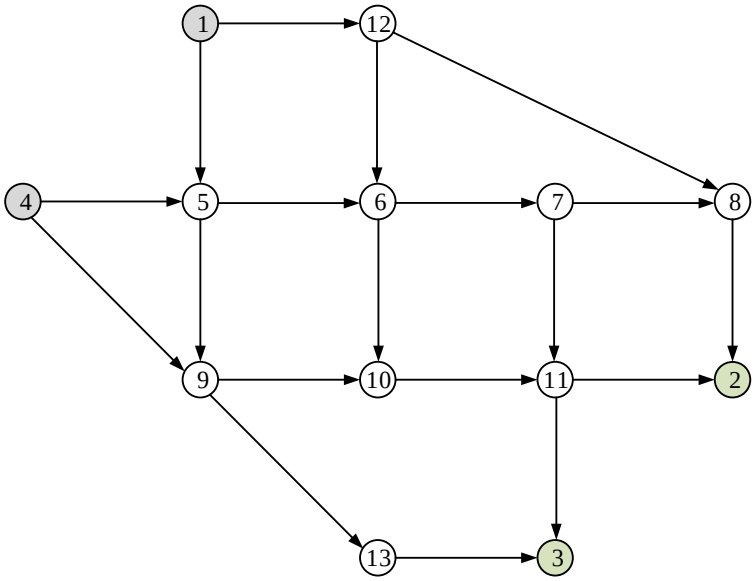

Fig. 10. The Nguyen and Dupius network for Example 5.

We set different fixed sample sizes and tested the convergence of the proposed extragradient method for the PDUO-RC problem. Fig. 11 provides the convergence curve for different fixed sample sizes. We can observe that the relative gap cannot reach 0.01 if the sample size is 10. However, the relative gap can be less than 0.01 if a larger sample size was adopted. The results presented in Fig. 11 indicate that using a larger sample size can improve the accuracy of the proposed extragradient method. We also can observe from Fig. 11 that the effect of the sample size on the relative gap is small for the first several iterations. This implies that we can initially use a small sample size to speed up the convergence and then increase the sample size to maintain the accuracy.

Table 1. The length of each link in the Nguyen and Dupius network

Link length (m)	450	600	600	750
Link	1-12	1-5	4-5	12-8
	7-8	4-9	5-6	
	7-11	5-9	6-7	
	9-13	6-10	9-10	
	8-2	11-2	11-3	
	10-11	12-6	13-3	

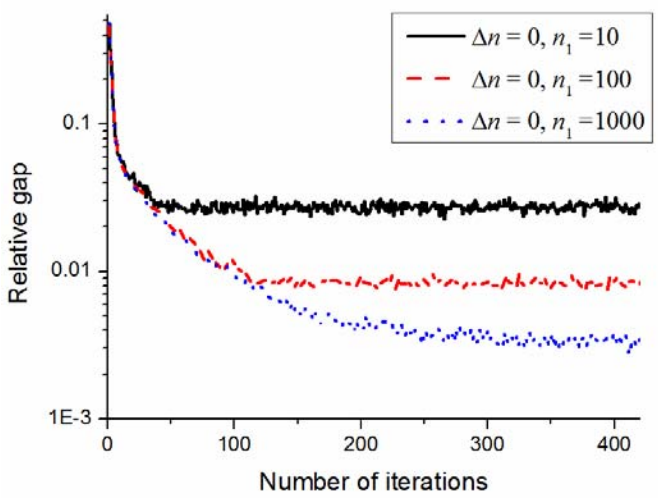

Fig. 11. The convergence of the modified extragradient method.

We solved the proposed PDUO-RC problem by using different sample size schemes and graphically show the relative gap against CPU time in Fig. 12. From this figure, we can observe that the relative gap decreases as CPU time increases. The value of gap function G_1 can reach 0.01 after 2.75 min and 0.40 min for a fixed sample size of 1000 and a variable sample size (i.e., $\Delta n = 10$ and $n_1 = 10$), respectively. This implies the variable sample size scheme outperforms the fixed sample size in terms of computational efficiency. Moreover, the black solid line is always above the red dashed line, meaning that the former gives a more accurate solution for a fixed running time. To sum up, the result also demonstrates that the variable sample size scheme can give a quicker and better solution than the traditional fixed sample size scheme.

Example 6: A test on the convergence of the modified route-swapping method for the PDUO-SRDTC problem using the test network in Example 4.

Traditionally, the DUO-SRDTC problems are formulated as VI problems (e.g., Huang and Lam, 2002; Szeto and Lo, 2004; Long et al., 2016b). Because the mapping functions of the VI problems for the DUE-SRDTC problems, i.e., route travel costs, are non-monotone, the existing solution algorithms cannot guarantee convergence (Long et al., 2016b), especially for large networks. We found that the PDUO-SRDTC problems are also very hard to be solved. In this example, we adopted the network in Fig. 8(b) to test the convergence of the modified route-swapping method for the studied PDUO-SRDTC problem. The design outflow capacities were 20 veh/interval for all links. The maximum degradations of outflow capacities were 1 veh/interval for links 1-4, 4-2, and 4-5, 5 veh/interval for link 1-5, and 5 veh/interval for link 5-3. The free-flow travel times were two intervals of link 4-5, and one interval for other links. The total OD demands of both OD pairs (1, 2) and (1, 3) were 160 veh and 200 veh, respectively. The parameters for the arrival time window were k_{rs}^{*} = 20 intervals and Δ_{rs} = 0 interval. By using various fixed sample sizes, we solved the PDUO-SRDTC problem by the route-swapping method and show the convergence curves are shown in Fig. 13. We can see that a larger sample size can improve the accuracy of the algorithm, which is similar to the convergence of the modified extragradient method for the studied PDUO-RC problem.

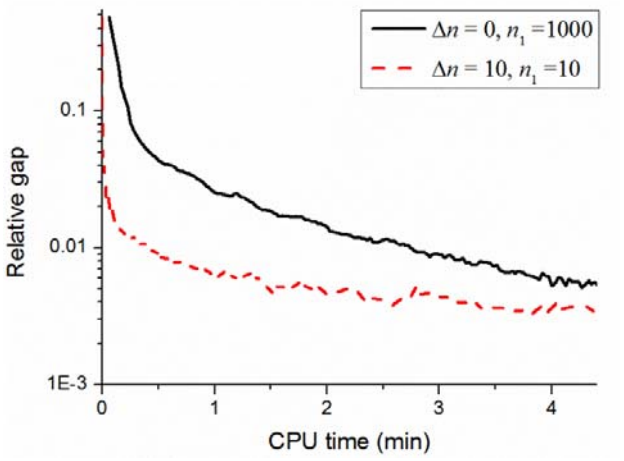

Fig. 12. The relative gap of the modified extragradient method against CPU time.

6. Conclusion

In this paper, we proposed a PDUO-SRDTC problem in a degradable transport network. In the degradable transport network, we assumed that each traveler chooses the path and departure time to minimize his/her own mean generalized route travel cost. As a special case of the PDUO-SRDTC problem, the PDUO-RC problem in a degradable transport network was also proposed. Both the PDUO-SRDTC and PDUO-RC problems were formulated as VI problems. An MC-SLTM was developed to capture both the effect of physical queues and the random evolution of traffic states during flow propagation and to evaluate the mean generalized route

travel costs for given route flow patterns. A modified route-swapping method and a modified extragradient method were respectively developed to solve the proposed PDUO-SRDTC problem and PDUO-RC problems.

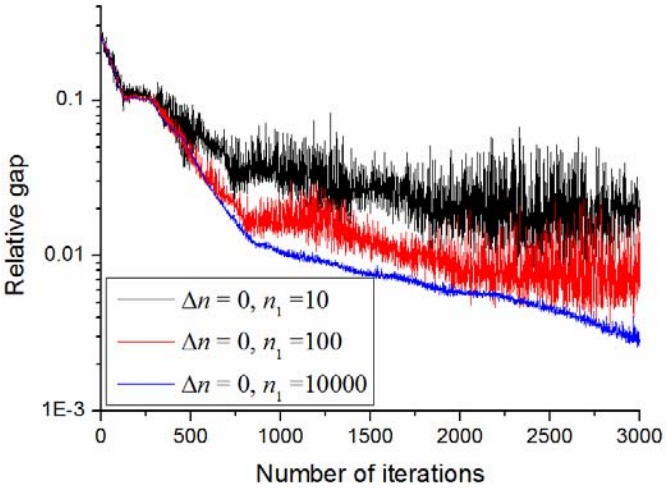

Fig. 13. The convergence of the modified route-swapping method.

Numerical examples were set up to test the performance of the proposed algorithms. The numerical results show that a larger sample size can improve the accuracy of the algorithm at the expense of computation time. The results also demonstrate that our proposed variable sample size scheme can obtain solutions with the same quality much quicker than fixed sample size scheme and that our scheme can obtain a better solution for a given computational time.

The proposed DTA models were further used to evaluate the effects of road network improvement and network degradation on network performance. Through different specific examples, we presented three interesting paradoxical phenomena that can occur in road networks: (1) the addition of a link may result in an increase in TSTC, (2) an improvement of road outflow capacity may result in an increase in TSTC, and (3) an increase of network degradation may result in an increase in TSTC. Moreover, the first two paradoxes may not be observed when queue spillback is ignored. These examples demonstrated that physical queue and network degradation must be taken into consideration in any policies aimed towards the reduction in TSTC.

In this paper, the PDUO principle was adopted as the travel choice principle. If travelers' perceptions of travel time were considered, we had a doubly stochastic dynamic traffic assignment problem (Szeto et al., 2011) and the travel choice principle can be referred as to the stochastic PDUO (SPDUO) principle. If the perception error equals zero, then a SPDUO DTA problem immediately becomes a PDUO DTA problem. Hence, the PDUO DTA problem is a special case of the PDUO DTA problem. This implies that the conclusions of the PDUO DTA problems in this paper can be generalized to the SPDUO DTA problems.

Acknowledgements

This work was jointly supported by the National Natural Science Foundation of China (71371026, 71431003, 71522001), a grant from the Research Grants Council of the Hong Kong Special Administrative Region, China (HKU 17207214), and the Fundamental Research Funds for the Central Universities (JZ2016HGPB0736). The authors are grateful to the two reviewers for their constructive comments.

References

Arnott, R., de Palma, A., Lindsey, R., 1990. Departure time and route choice for the morning commute. *Transportation Research Part B*, 24(3), 209-228.

Bie, J., Lo, H. K., 2010. Stability and attraction domains of traffic equilibria in a day-to-day dynamical system formulation. *Transportation Research Part B*, 44(1), 90-107.

Carey, M., Ge, Y.E., 2012. Comparison of methods for path inflow reassignment for dynamic user equilibrium. *Networks and Spatial Economics*, 12(3), 337-376.

Carey, M., Srinivasan, A., 1993. Externalities, average and marginal costs, and tolls on congested networks with time-varying flows. *Operations Research*, 41(1), 217-231.

Chen, H.K., Hsueh, C.F., 1998. Discrete-time dynamic user-optimal departure time/route choice model. Journal of Transportation Engineering, 124(3), 246-254.

Chow, A.H.F., Li, S., Szeto, W.Y., and Wang, D.Z.W., 2015. Modelling urban traffic dynamics based upon the variational formulation of kinematic waves. *Transportmetrica B*, 3(3), 169–191.

Daganzo, C.F., 1995. The cell transmission model, Part II: Network traffic. *Transportation Research Part B*, 29(2), 79-93.

Friesz, T.L., Bernstein, D., Smith, T.E., Tobin, R.L., Wie, B., 1993. A variational inequality formulation of the dynamic networks user equilibrium problem. *Operations Research*, 41(1), 179-191.

Fosgerau, M., 2010. On the relation between the mean and variance of delay in dynamic queues with random capacity and demand. *Journal of Economic Dynamics and Control* 34(4), 598–603.

Ge, Y.E., Sun, B.R., Zhang, H.M., Szeto, W.Y., Zhou, X., 2015a. A comparison of dynamic user optimal states with zero, fixed and variable tolerances. *Networks and Spatial Economics*, 15(3), 583-598.

Ge, Y.E., Xu, C.F., Szeto, W.Y., Sun, B.R., and Zhang, H.M., 2015b. Investigating freeway traffic hypercongestion between an on-ramp and its immediate upstream off-ramp. *Transportmetrica A*, 11(3), 187-209.

Han, K., Friesz, T.L., Yao, T., 2013a. A partial differential equation formulation of Vickrey's bottleneck model, part II: Numerical analysis and computation. *Transportation Research Part B*, 49, 75-93.

Han, K., Friesz, T.L., Yao, T., 2013b. Existence of simultaneous route and departure choice dynamic user

equilibrium. *Transportation Research Part B*, 53, 17-30.

Han, K., Friesz, T.L., Szeto, W.Y., and Liu, H.-C., 2015. Elastic demand dynamic network user equilibrium: Formulation, existence and computation. *Transportation Research Part B*, 81, 183-209.

Han, K., Piccoli, B., Szeto, W.Y., 2016. Continuous-time link-based kinematic wave model: Formulation, solution existence, and well-posedness, *Transportmetrica B*, 4(3), 187-222.

Han, K., Szeto, W.Y., and Friesz, T.L., 2015. Formulation, existence, and computation of boundedly rational dynamic user equilibrium with fixed or endogenous user tolerance. *Transportation Research Part B*, 79, 16-49.

Huang, H.J., Lam, W.H.K., 2002. Modeling and solving the dynamic user equilibrium route and departure time choice problem in network with queues. *Transportation Research Part B*, 36(3), 253-273.

Jiang, Y., Szeto, W.Y., Long, J.C., Han, K., 2016. Multi-class dynamic traffic assignment with physical queues: Intersection-movement-based formulation and paradox. *Transportmetrica A*, 12(10) 878-908.

Jin, W. L., 2007. A dynamical system model of the traffic assignment problem. *Transportation Research Part B*, 41(1), 32-48.

Korpelevich, G.M., 1976. The extragradient method for finding saddle points and other problems. *Matecon*, 12, 747-756.

Kuwahara, M., 1990. Equilibrium queuing patterns at a two-tandem bottleneck during the morning peak. *Transportation Science*, 24(3), 217-229.

Kuwahara, M., Akamatsu, T., 1997. Decomposition of the reactive dynamic assignments with queues for a many-to-many origin-destination pattern. *Transportation Research Part B*, 31(1), 1-10.

Kuwahara, M., Akamatsu, T., 2001. Dynamic user optimal assignment with physical queues for a many-to-many OD pattern. *Transportation Research Part B*, 35(5), 461-479.

Li, X.G., Lam, W.H.K., Shao, H., Gao, Z.Y., 2015. Dynamic modelling of traffic incident impacts on network reliability. *Transportmetrica A*, 11(9), 856-872.

Lighthill, M.H., Whitham, G.B., 1955. On kinematics wave II: A theory of traffic flow on long crowed roads. *Proceedings of the Royal Society*, London, Series A 229(1178), 317-345.

Lim, Y., Heydecker, B., 2005. Dynamic departure time and stochastic user equilibrium assignment. *Transportation Research Part B*, 39(2), 97-118.

Lindsey, R., 2004. Existence, uniqueness, and trip cost function properties of user equilibrium in the bottleneck model with multiple user classes. *Transportation Science*, 38(3), 293-314.

Liu, Z., Meng, Q., 2013. Distributed computing approaches for large‐scale probit‐based stochastic user equilibrium problems. *Journal of Advanced Transportation*, 47(6), 553-571.

Lo, H. K., Luo, X. W., Siu, B. W., 2006. Degradable transport network: travel time budget of travelers with heterogeneous risk aversion. *Transportation Research Part B*, 40(9), 792-806.

Lo, H. K., Tung, Y. K., 2003. Network with degradable links: capacity analysis and design. *Transportation Research Part B*, 37(4), 345-363.

Lo, H.K., Szeto, W.Y., 2002. A cell-based variational inequality formulation of the dynamic user optimal assignment problem. *Transportation Research Part B*, 36(5), 421-443.

Long, J.C., Chen, J.X., Szeto, W.Y., Shi, Q., 2016a. Link-based system optimum dynamic traffic assignment problems with environmental objectives. *Transportation Research Part D*, DOI: 10.1016/j.trd.2016.06.003.

Long, J.C., Gao, Z.Y., Szeto, W.Y., 2011. Discretised link travel time models based on cumulative flows: Formulation and properties. *Transportation Research Part B*, 45(1), 232–254.

Long, J.C., Huang, H.J., Gao, Z.Y., 2013a. Discretised route travel time models based on cumulative flows. *Journal of Advanced Transportation*, 47(1):105-125.

Long, J.C., Huang H.J., Gao, Z.Y., Szeto, W.Y., 2013b. An intersection-movement-based dynamic user optimal route choice problem. *Operations Research*, 61 (5), 1134-1147.

Long, J.C., Szeto, W.Y., Gao, Z.Y., Huang, H.J., Shi, Q., 2016b. The nonlinear equation system approach to solving dynamic user optimal simultaneous route and departure time choice problems. *Transportation Research Part B*, 83, 179-206.

Long, J.C., Szeto, W.Y., Huang, H.J., Gao, Z.Y., 2015a. An intersection-movement-based stochastic dynamic user optimal route choice model for assessing network performance. *Transportation Research Part B*, 74, 182-217.

Long, J.C., Szeto, W.Y., Shi, Q., Gao, Z.Y., and Huang, H.J., 2015b. A nonlinear equation system approach to the dynamic stochastic user equilibrium simultaneous route and departure time choice problem. *Transportmetrica A*, 11(5), 388-419.

Meng, Q., Khoo, H.L. 2012. A computational model for the probit-based dynamic stochastic user optimal traffic assignment problem. *Journal of Advanced Transportation*, 46(1), 80-94.

Meng, Q., Liu, Z., 2012. Mathematical models and computational algorithms for probit-based asymmetric stochastic user equilibrium problem with elastic demand. *Transportmetrica*, 8(4), 261-290.

Merchant, D.K, Nemhauser, G.L., 1978a. A model and an algorithm for the dynamic traffic assignment. *Transportation Science*, 12(3), 183-199.

Merchant, D.K, Nemhauser, G.L., 1978b. Optimality conditions for a dynamic traffic assignment model. *Transportation Science*, 12(3), 200-207.

Mounce, R., Carey, M., 2011. Route swapping in dynamic traffic networks. *Transportation Research Part B*, 45 (1), 102-111.

Mun, J.S., 2007. Traffic performance models for dynamic traffic assignment: An assessment of existing models, *Transport Reviews*, 27 (2), 231-249.

Newell, G.F., 1993. A simplified theory on kinematic wave in highway traffic, Part I: General theory; Part II: Queuing at freeway bottlenecks; Part III: Multi-destination flows. *Transportation Research Part B*, 27(4), 281-314.

Nie, X., Zhang, H., 2005. A comparative study of some macroscopic link models used in dynamic traffic assignment. *Networks and Spatial Economics*, 5(1), 89-115.

Nie, Y., 2011. A cell-based Merchant-Nemhauser model for the system optimum dynamic traffic assignment problem. *Transportation Research Part B*, 45(2), 329-342.

Nie, Y., Zhang, H.M. 2010. Solving the dynamic user optimal assignment problem considering queue spillback. *Networks and Spatial Economics*, 10, 49-71.

Panicucci, B., Pappalardo, M., Passacantando, M., 2007. A path-based double projection method for solving the asymmetric traffic network equilibrium problem. *Optimization Letters*, 1(2), 171-185.

Qian, Z.S., Xiao, F.E., Zhang, H.M., 2012. Managing morning commute traffic with parking. *Transportation Research Part B*, 46(7), 894-916.

Ran, B., Boyce, D.E., 1996. Modeling Dynamic Transportation Network: An Intelligent Transportation System Oriented Approach. Springer, Heidelberg.

Richards, P.I., 1956. Shock waves on the highway. *Operations Research*, 4(1), 42-51.

Siu, B.W.Y., Lo, H.K., 2013. Punctuality-based departure time scheduling under stochastic bottleneck capacity: formulation and equilibrium. *Transportmetrica B*, 1(3), 195-225.

Smith, M.J., 1984. The stability of a dynamic model of traffic assignment—an application of a method of Lyapunov. *Transportation Science*, 18(3), 245-252.

Sumalee, A., Zhong, R.X., Pan, T.L., Szeto, W.Y., 2011. Stochastic cell transmission model (SCTM): a stochastic dynamic traffic model for traffic state surveillance and assignment. *Transportation Research Part B*, 45(3), 507-533.

Szeto, W.Y., Jiang, Y., 2014. Transit assignment: Approach-based formulation, extragradient method, and paradox. *Transportation Research Part B*, 62, 51-76.

Szeto, W.Y., Jiang, Y., Sumalee, A., 2011. A cell-based model for multi-class doubly stochastic dynamic traffic assignment. *Computer-Aided Civil and Infrastructure Engineering*, 26(8), 595-611.

Szeto, W.Y., Lo, H.K., 2004. A cell-based simultaneous route and departure time choice model with elastic demand. *Transportation Research Part B*, 38(7), 593-612.

Szeto, W.Y., Lo, H.K., 2006. Dynamic traffic assignment: Properties and extensions. *Transportmetrica*, 2(1),

31-52.

Szeto, W.Y., Wong, S.C., 2012. Dynamic traffic assignment: model classifications and recent advances in travel choice principles. *Central European Journal of Engineering*, 2(1), 1-18.

Tian, L.J., Huang, H.J., Gao, Z.Y., 2012. A cumulative perceived value-based dynamic user equilibrium model considering the travelers' risk evaluation on arrival time. *Networks and Spatial Economics*, 12(4), 589-608.

Vickrey, W.S., 1969. Congestion theory and transport investment. *American Economic Review*, 59(2), 251-261.

Xiao, L.L., Huang, H.J., Liu, R.H., 2015. Congestion behavior and tolls in a bottleneck model with stochastic capacity. *Transportation Science*, 49(1), 46-65.

Yook, D., Heaslip, K., 2016. Acceleration of double-projection method in asymmetrically formulated traffic assignment. *Journal of Computing in Civil Engineering*, 30(6), 04016025.

Yperman, I., 2007. The link transmission model for dynamic network loading. Ph.D. dissertation, Katholieke Universiteit Leuven, Leuven, Belgium.

Zhang, X.N., Lam, W.H.K., Huang, H.J., 2008. Braess's paradoxes in dynamic traffic assignment with simultaneous departure time and route choices. *Transportmetrica*, 4(3), 209-225.

Zheng, H., Chang, Y.C., 2011. A network flow algorithm for the cell-based single-destination system optimal dynamic traffic assignment problem. *Transportation Science*, 45(1), 121-137.

Zhu, F., Ukkusuri, S.V., 2013. A cell based dynamic system optimum model with non-holding back flows. *Transportation Research Part C*, 36, 367-380.

Ziliaskopoulos, A.K., 2000. A linear programming model for the single destination system optimum dynamic traffic assignment problem. *Transportation Science*, 34(1), 37-44.